A new strategy for searching for gravitational lens pairs formed by a cosmic string: theory and observations

Sazhina O.S.
(SAI MSU)

QUARKS-2024

with
I. Bulygin
M. Safonova
M. Sazhin
P. Hasan
F. Sutaria

Cosmic string in cosmology

CS as possible cosmological objects were first predicted by T. W.B. Kibble (1976) (T.W.B. Kibble, J. Phys. A Math. Gen. **9**, 1387 (1976); M.B. Hindmarsh, T.W.B. Kibble, (1994). arXiv:hep-ph/9411342)

and were actively studied in works by Ya. B. Zel'dovich (1980), A. Vilenkin (1981) and others (Y.B. Zeldovich, MNRAS 192, 663 (1980); A. Vilenkin, Phys. Rev. D 23, 852 (1981); A. Vilenkin, ApJ 289, L51 (1984); F. Bernardeau, J.-P. Uzan, Phys. Rev. D 63(023004), 023005 (2001); A.A. de Laix, T. Vachaspati, Phys. Rev. D 54, 4780 (1996); D.P. Bennett, F.R. Bouchet, High resolution simulations of cosmic string evolution I: network evolution. Phys. Rev. D 41, 2408 (1990); B. Allen, E.P.S. Shellard, Cosmic string evolution: a numerical simulation. Phys. Rev. Lett. 64, 119 (1990); C.J.A.P. Martins, E.P.S. Shellard, Fractal properties and small scale structure of cosmic string networks. Phys. Rev. D 73, 043515 (2005). arXiv:astro-ph/0511792; C. Ringeval, M. Sakellariadou, F.R. Bouchet, Cosmological evolution of cosmic string loops. JCAP 0702, 023 (2007). arXiv:astro-ph/0511646).

In particular, the role of CS in the formation of gravitational-lens images was shown by A. Vilenkin (Phys. Rev. D **23**, 852 (1981)), and the mechanism of generation of CMB anisotropy by N. Kaiser, A. Stebbins (Nature **310**, 391 (1984)).

THEORY:

Theory of gravitational lensing on a curved cosmic string. Bulygin, I.I., Sazhin, M.V. & Sazhina, O.S. Eur. Phys. J. C 83, 844 (2023);

arXiv:2306.09062

OBSERVATIONS:

Deep Photometry of Suspected Gravitational Lensing Events: Potential Detection of a Cosmic String. Safonova, M., Bulygin, I.I., Sazhina, O.S., Sazhin, M.V., Hasan, P., Sutaria, F. Accepted at the Bulletin de la Société Royale des Sciences de Liège (2023);

arXiv:2309.11831v1

Optical analysis of a CMB cosmic string candidate. Sazhina, O.S., Scognamiglio, D., Sazhin, M.V., Capaccioli, M. MNRAS, V. 485, Iss.2, P. 1876–1885 (2019);

arXiv:1902.08156

OVERVIEW:

Space fabric wrinkles: history of observational searches for exotic structures in the Universe. Sazhin, M.V., Sazhina, O.S. Riv. Nuovo Cim. 44, 397–451 (2021). https://doi.org/10.1007/s40766-021-00022-x

M. V. Sazhin
(1951 – 2023)

Cosmic string as topological object

The field theory approach:

$$U(1), \qquad \varphi = A(r)e^{i\theta(\varphi)}$$

The simplest model of CS formation: phase transitions in the early Universe with symmetry breaking. Violation of the simplest symmetry U(1) admits the CS as a topologically stable solution. (Topological stability means the continuity of the scalar field when rotating by 2π around a certain point.) The appropriate solution is a new stable field vacuum at this point. The geometric location of all points of such a vacuum is a CS.

The effective theory approach:

Nambu-Goto action for infinitely long bosonic CS

$$S = \mu \int d^2\xi\sqrt{-\det\gamma_{ab}} + O\left({R_{\mathrm{CS}}}^{-1}\right)$$

← for a one-dimensional CS the action is determined by the area of the world sheet swept by it with an accuracy of the first order of curvature.

$$S_1 = \mu\alpha_1 \int d^2\xi\sqrt{-\det\gamma_{ab}} \cdot \frac{{r_0}^2}{{R_{\mathrm{CS}}}^{(2)}}$$

$$\xi_1 = t, \quad \xi_2 = \sigma$$
$$X^0 = t, \qquad \boldsymbol{X} = X^i$$

$$\begin{aligned} -\det \gamma_{ab} &= \left(g_{\mu\nu}\partial_1 X^\mu \partial_2 X^\nu\right)^2 - \left(g_{\mu\nu}\partial_1 X^\mu \partial_1 X^\nu\right)\cdot\left(g_{\mu\nu}\partial_2 X^\mu \partial_2 X^\nu\right) \\ &= -\gamma \end{aligned}$$

Linear density $\dfrac{dm}{d\sigma} = A(\sigma) = \dfrac{1}{\sqrt{1-\left(\dfrac{\partial \boldsymbol{X}}{\partial t}\right)^2}}\left|\dfrac{\partial \boldsymbol{X}}{\partial \sigma}\right| = 1$

We need that the equations of motion in the physical coordinates $\boldsymbol{X}$ have a physical meaning. With this calibration, the equations of motion become wave equations.

Wave equation $\partial_t{}^2 \boldsymbol{X} - \partial_\sigma{}^2 \boldsymbol{X} = 0$

$$T_{\mu\nu} = -2\frac{\delta\left(\sqrt{-g}\cdot\mathcal{L}_M\right)}{\delta g^{\mu\nu}} = \mu\int d\sigma \frac{1}{\sqrt{-\gamma}}\frac{\delta\gamma}{\delta g^{\mu\nu}}\cdot\delta^{(3)}\left(x - \boldsymbol{X}(\sigma,t)\right)$$

$$\frac{1}{\sqrt{-\gamma}}\frac{\delta\gamma}{\delta g^{\mu\nu}} = -\frac{1}{A(\sigma)}\partial_\sigma X_\mu \partial_\sigma X_\nu + A(\sigma)\partial_t X_\mu \partial_t X_\nu = \partial_t X_\mu \partial_t X_\nu - \partial_\sigma X_\mu \partial_\sigma X_\nu$$

$$E = \int d^3x T^{00} = \mu\int d\sigma = \mu\cdot\Delta\sigma$$

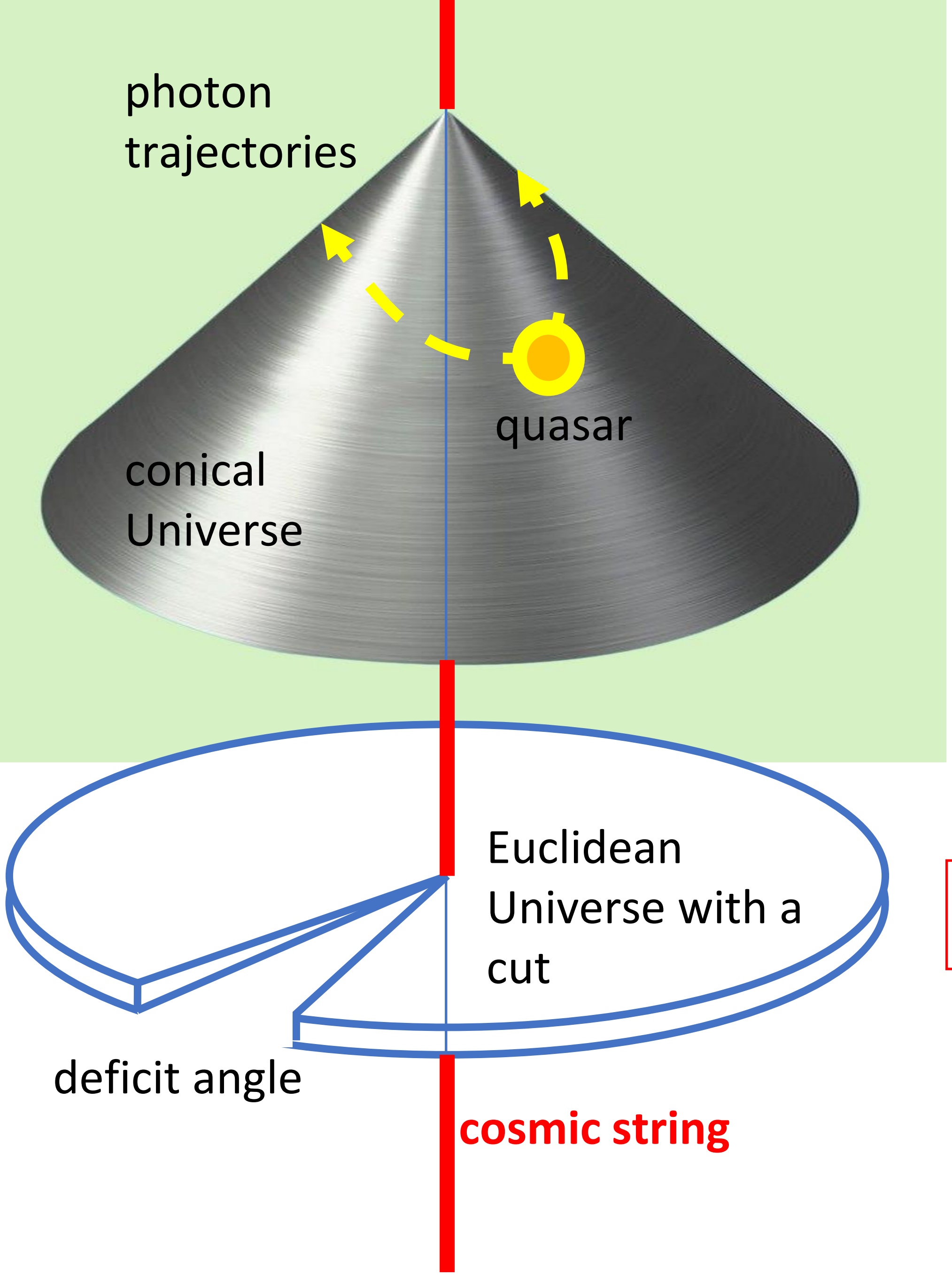

$$T^{\mu\nu}(\boldsymbol{x}) = \mu \int d\sigma(\partial_t X^\mu \partial_t X^\nu - \partial_\sigma X^\mu \partial_\sigma X^\nu) \cdot \delta^{(3)}(\boldsymbol{x} - \boldsymbol{X}(\sigma, t))$$

$$T^{00} = -T^{zz} = \mu\delta(x)\delta(y) = \frac{\mu}{2\pi r}\delta(r)$$

$$h_{\mu\nu}(x) = 4G \int d\boldsymbol{x}' \frac{S_{\mu\nu}}{|\boldsymbol{x} - \boldsymbol{x}'|}$$

$$\frac{d^2x^i}{dt^2} = -\left(\Gamma_{\mu\nu}{}^i - \Gamma_{\mu\nu}{}^0 \frac{dx^i}{dt}\right)\frac{dx^\mu}{dt}\frac{dx^\nu}{dt}, \boldsymbol{x} = (x \quad y \quad z)$$

$$\Delta h_{11} = 16\pi G T^{00}, \qquad \Delta h_{22} = 16\pi G T^{00}$$

$$ds^2 = dt^2 - dz^2 - dr^2 - r^2(1 - 4G\mu)^2 d\varphi^2$$

A. Vilenkin, 1980

$$\varphi' = \varphi(1 - 4G\mu), \qquad \varphi' \in [0, 2\pi - \Delta\theta],$$

$$\Delta\theta = 8\pi G\mu/c^2$$

All effect are related with angles (iwhen re-defining the angle, we get a flat metric). Flat space with cut is the cone.

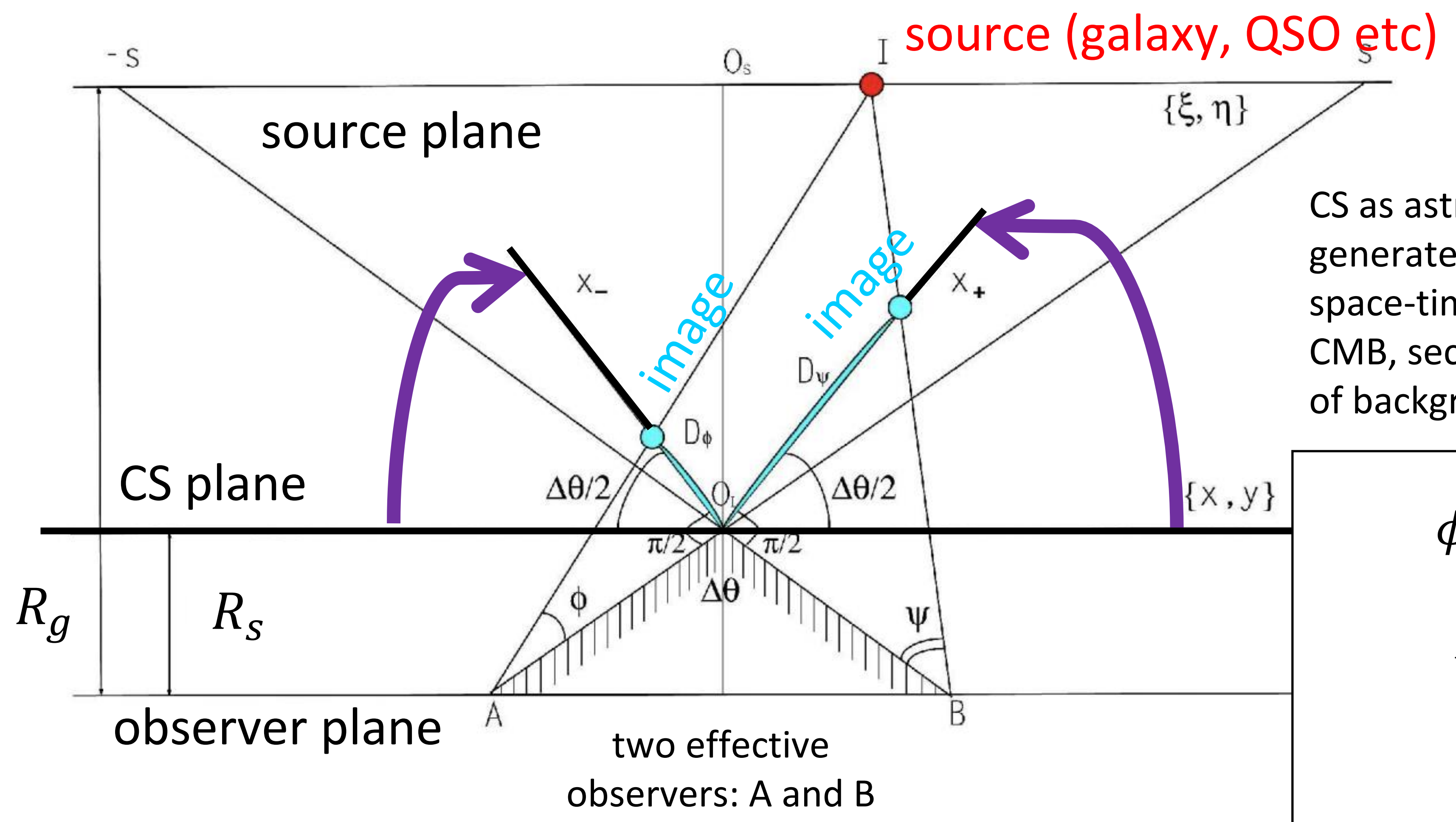

CS as astrophysical object (being invisible itself) generate the observable effects due to the conical space-time. First one is specific anisotropy in CMB, second one is specific gravitational lensing of background sources.

$$\phi = -\eta + 4\pi \cdot G\mu \left(1 - \frac{R_s}{R_g}\right)$$

$$\psi = \eta + 4\pi \cdot G\mu \left(1 - \frac{R_s}{R_g}\right)$$

$$I_1(\eta, \xi) = \begin{cases} I(\eta - \theta_E/2, \xi), \eta > -\theta_E \\ 0, \eta \leq -\theta_E \end{cases}$$

$$I_2(\eta, \xi) = \begin{cases} I(\eta + \theta_E/2, \xi), \eta < \theta_E \\ 0, \eta \geq \theta_E \end{cases}$$

Approximation of geometric optics.
A locally flat metric.

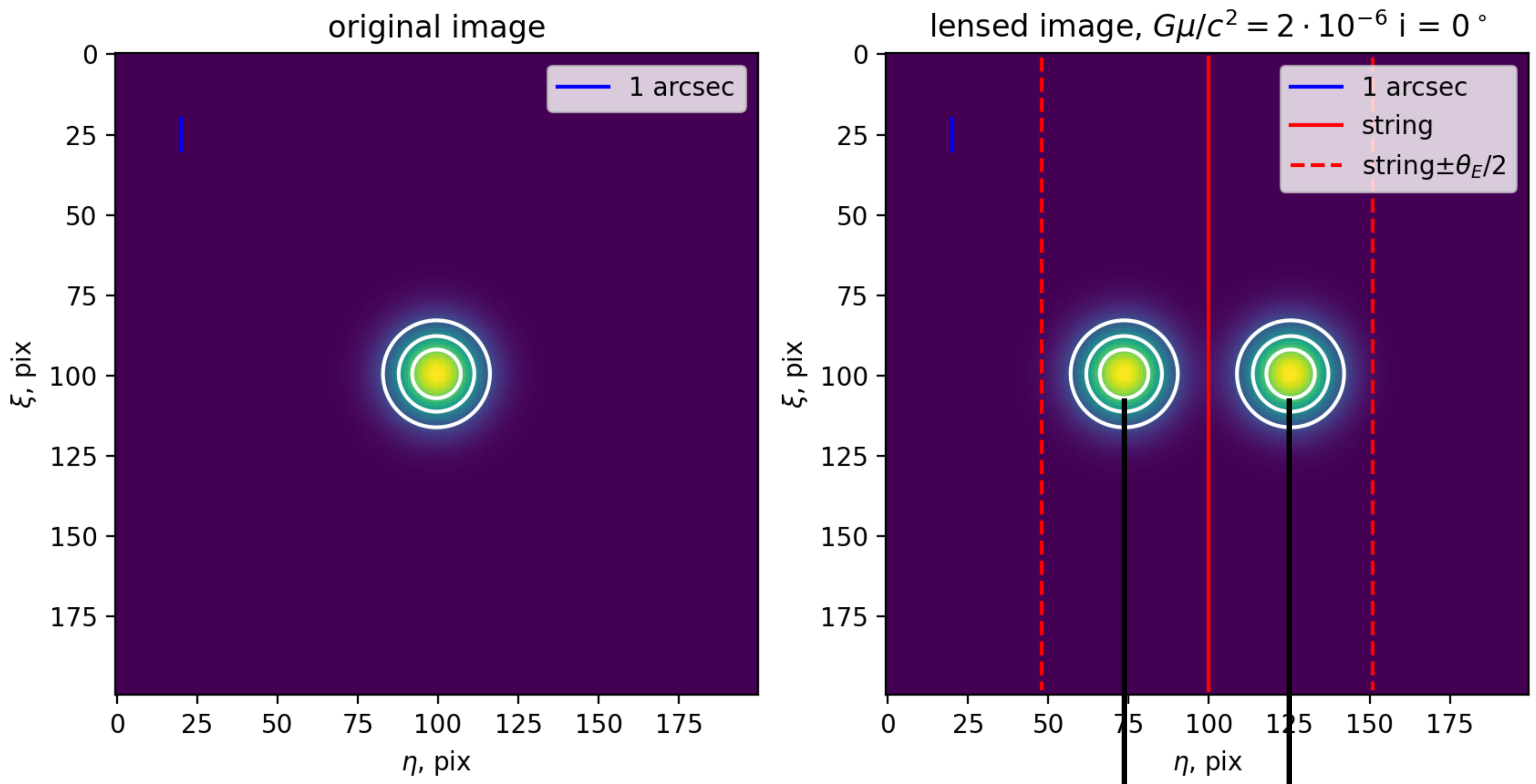

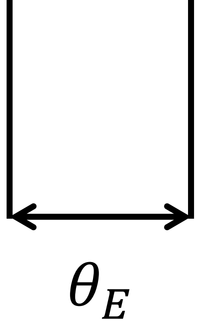

$$I_{1+2}(\eta,\xi) = \begin{cases} I(\eta+\theta_E/2,\xi), \eta < -\theta_E \\ I(\eta+\theta_E/2,\xi) + I(\eta-\theta_E/2,\xi), |\eta| \le \theta_E \\ I(\eta-\theta_E/2,\xi), \eta > \theta_E \end{cases}$$

$$\theta_E = \Delta\theta\left(1 - \frac{R_s}{R_g}\right)$$

CS with inclination

$$R_s(\xi) = \frac{R_s}{\cos\xi + \operatorname{tg} i \sin\xi} \approx \frac{R_s}{1 + \xi \operatorname{tg} i}$$

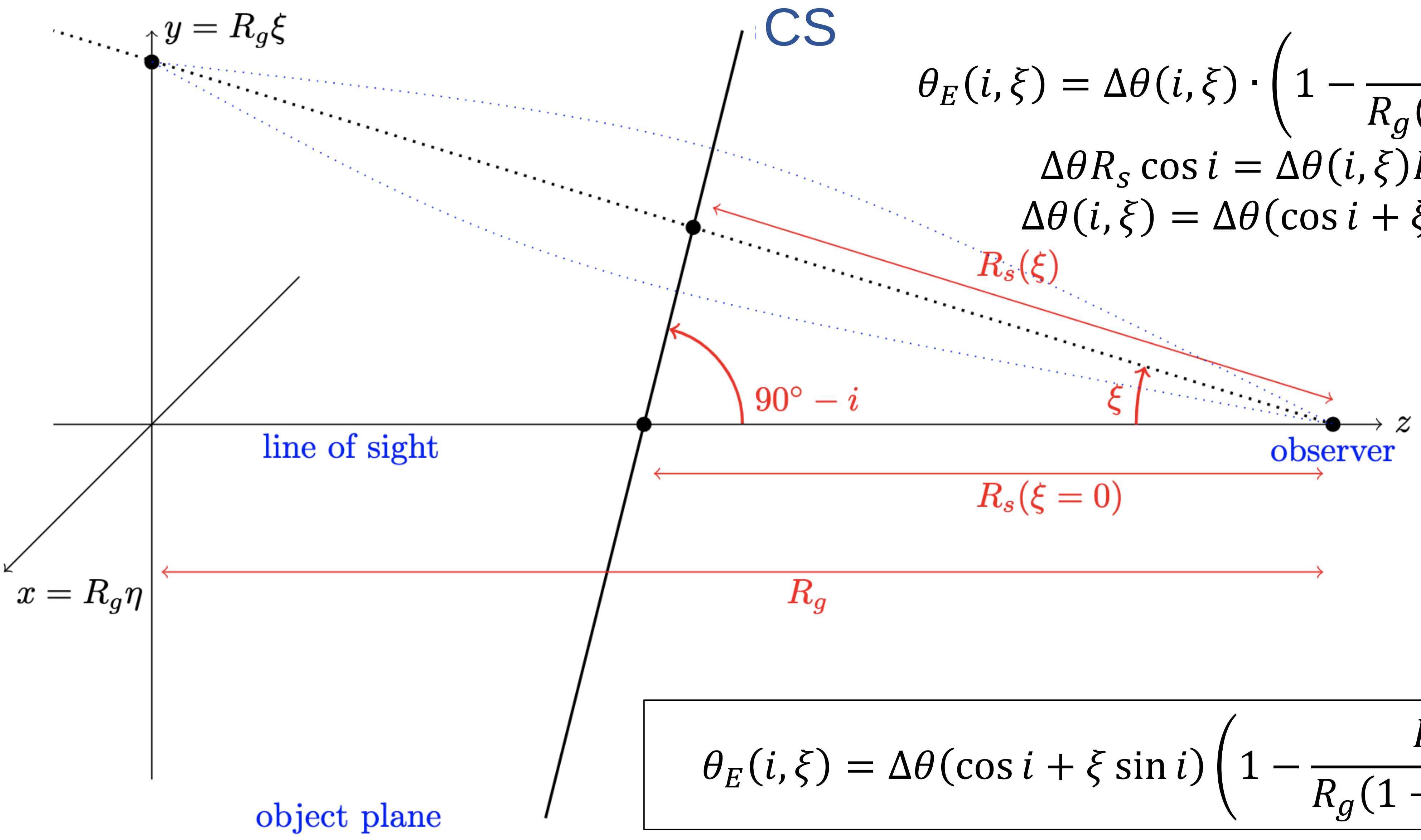

$$\theta_E(i,\xi) = \Delta\theta(i,\xi) \cdot \left(1 - \frac{R_s}{R_g(1 + \xi \operatorname{tg} i)}\right)$$

$$\Delta\theta R_s \cos i = \Delta\theta(i,\xi) R_s(\xi)$$

$$\Delta\theta(i,\xi) = \Delta\theta(\cos i + \xi \sin i)$$

$$\theta_E(i,\xi) = \Delta\theta(\cos i + \xi \sin i)\left(1 - \frac{R_s}{R_g(1 + \xi \operatorname{tg} i)}\right) \neq \text{const}$$

CS with inclination

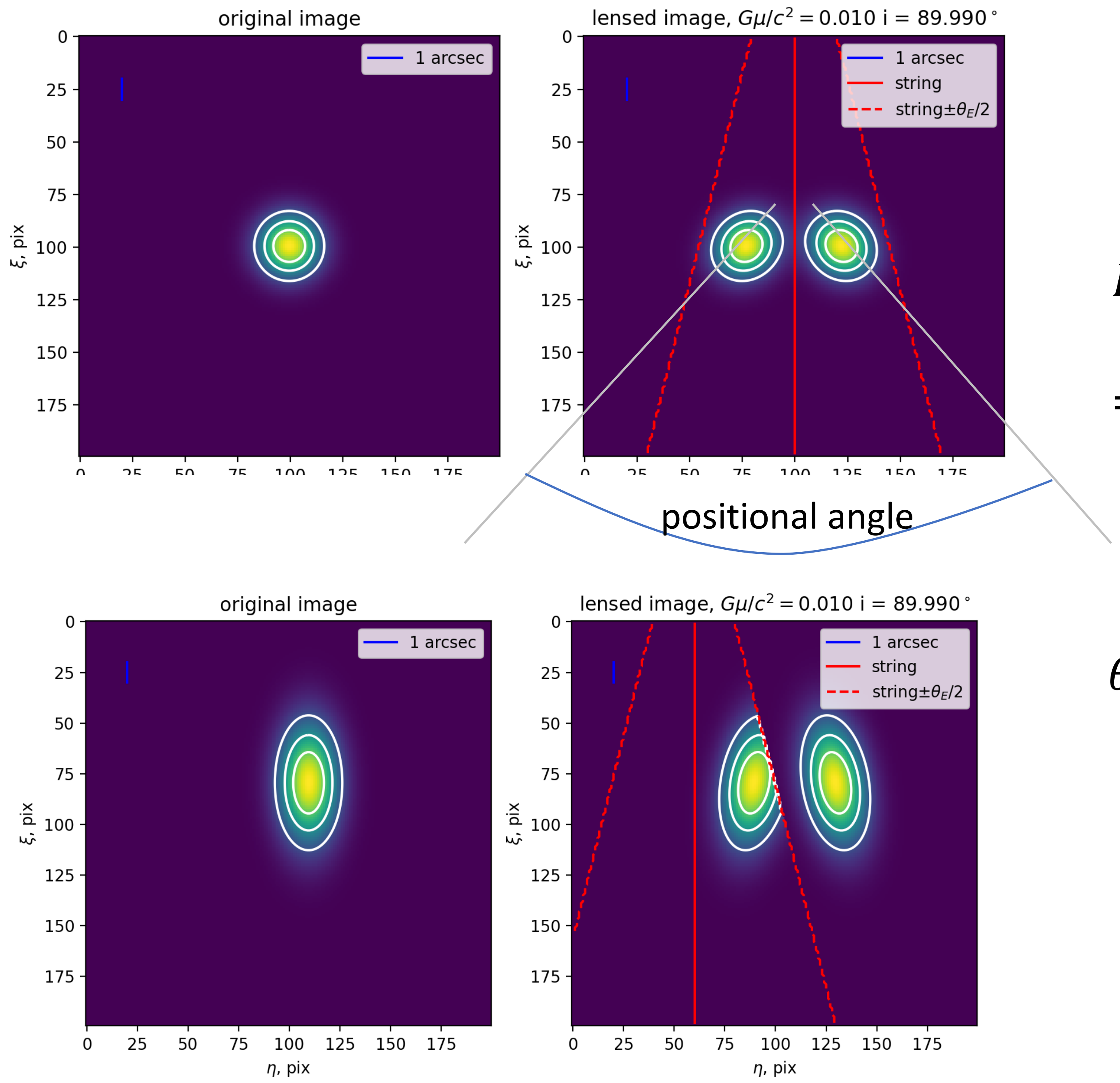

$$I_{1+2}(\eta, \xi) = \begin{cases} I(\eta + \theta_E/2, \xi), \eta < -\theta_E \\ I(\eta + \theta_E/2, \xi) + I(\eta - \theta_E/2, \xi), |\eta| \leq \theta_E \\ I(\eta - \theta_E/2, \xi), \eta > \theta_E \end{cases}$$

$$\theta_E = \Delta\theta(\cos i + \xi \sin i)\left(1 - \frac{R_s}{R_g(1 + \xi \operatorname{tg} i)}\right)$$

CS with bend

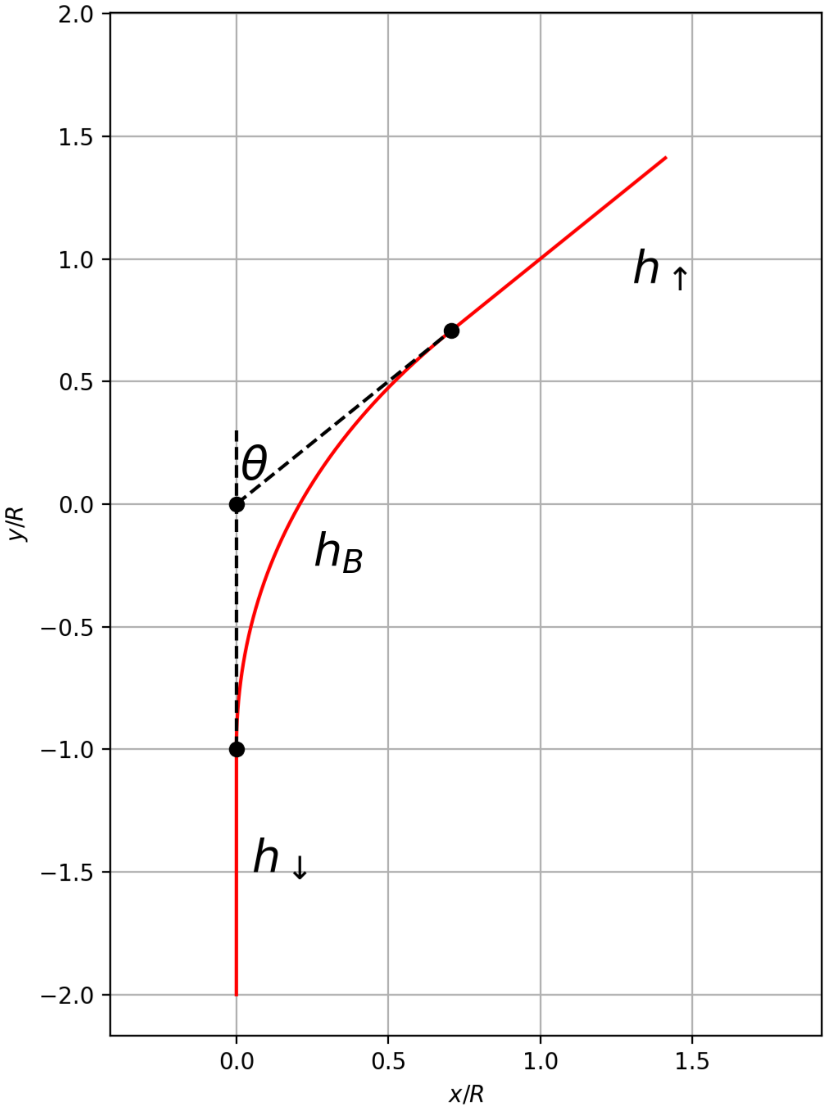

$$\begin{cases} X^1(s) = x(s) = \begin{cases} 0, s \in (-\infty, -R) \\ \dfrac{R\sin\theta}{4}\left(1+\dfrac{s}{R}\right)^2, s \in [-R, R] \\ s\sin\theta,\ s \in (R, +\infty) \end{cases} \\ X^2(s) = y(s) = \begin{cases} 0, s \in (-\infty, -R) \\ \dfrac{R\cos\theta}{4}\left(1+\dfrac{s}{R}\right)^2 - \dfrac{R}{4}\left(1-\dfrac{s}{R}\right)^2, s \in [-R, R] \\ s\cos\theta,\ s \in (R, +\infty) \end{cases} \\ X^3(s) = z(s) = R_g - R_s \end{cases}$$

$$T_{\mu\nu}(\boldsymbol{x}) = \mathcal{F}^{-1}\left(\mu \int_{-\infty}^{\infty} d\sigma \exp(-i\,\boldsymbol{k}\,\boldsymbol{X}) \cdot \left(\partial_t X_\mu \partial_t X_\nu - \partial_\sigma X_\mu \partial_\sigma X_\nu\right)\right)$$

$$\frac{d\sigma}{ds} = \rho(s) = \sqrt{x'(s)^2 + y'(s)^2 + z'(s)^2} =$$

$$= \begin{cases} 1, s \in (-\infty, -R) \\ \sqrt{\cos^2\theta/2 + (s/R)^2 \sin^2\theta/2}, s \in [-R, R] \\ 1, s \in (R, +\infty) \end{cases}$$

CS with bend

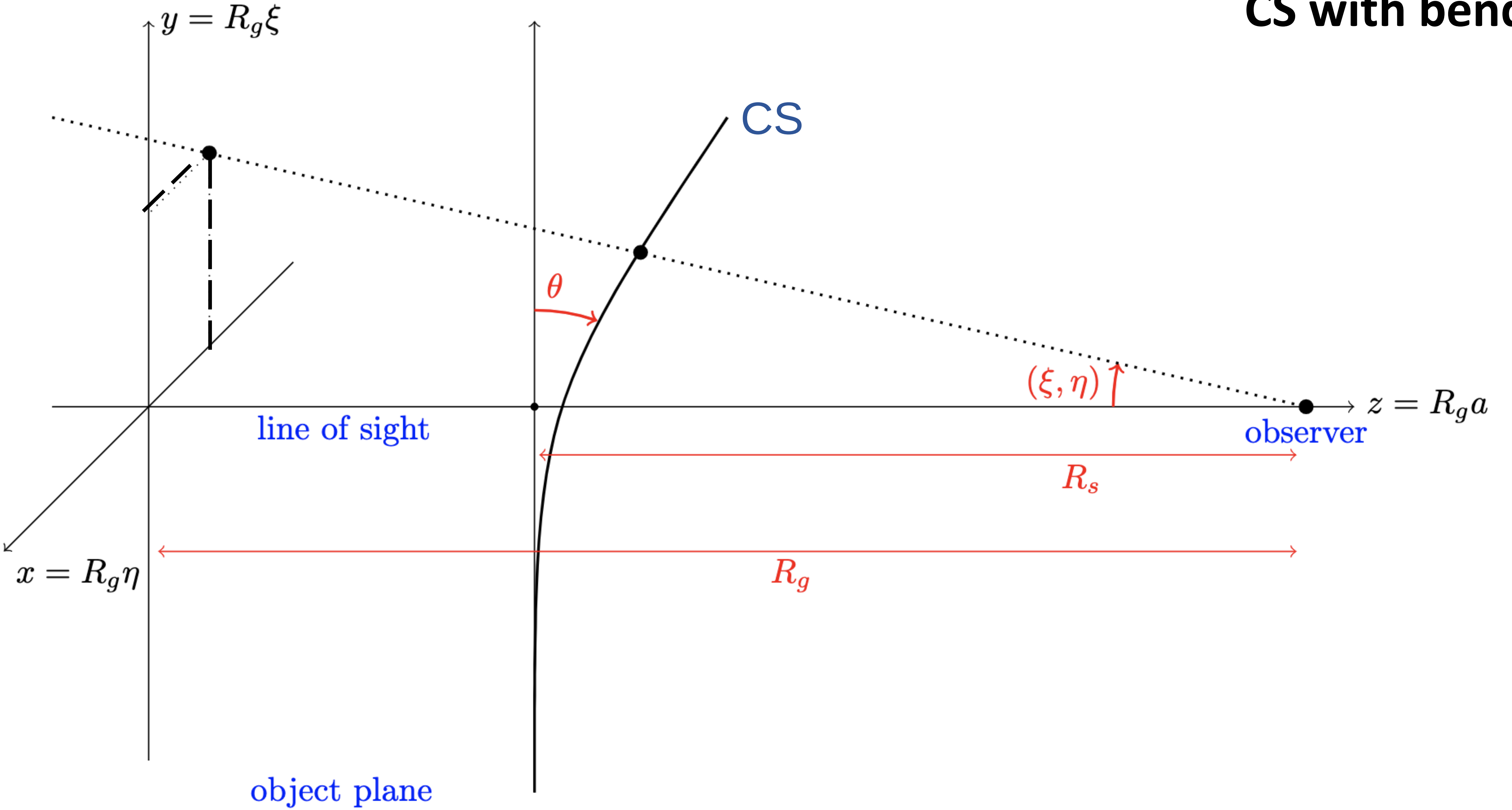

$y = R_g\xi$
CS
θ
(ξ, η)
$z = R_g a$
line of sight
observer
R_s
$x = R_g\eta$
R_g
object plane

CS with bend

$$\frac{d\sigma}{ds} = \rho(s) = \sqrt{x'(s)^2 + y'(s)^2 + z'(s)^2} = \begin{cases} 1, s \in (-\infty, -R) \\ \sqrt{cos^2\, \theta/2 + (s/R)^2 sin^2\theta/2}, s \in [-R, R] \\ 1, s \in (R, +\infty) \end{cases}$$

$$T^{\mu\nu}(\boldsymbol{x}) = \mu \int d\sigma (\partial_t X^\mu \partial_t X^\nu - \partial_\sigma X^\mu \partial_\sigma X^\nu) \cdot \delta^{(3)}\big(\boldsymbol{x} - \boldsymbol{X}(\sigma, t)\big)$$

$$T^{00}(\boldsymbol{x}) = \mu \int_{-\infty}^{-R} ds \delta^{(3)}\big(\boldsymbol{x} - \boldsymbol{X}(s)\big)$$

$$+ \mu \int_{-R}^{R} ds \sqrt{cos^2\, \theta/2 + (s/R)^2 sin^2\theta/2}\, \delta^{(3)}\big(\boldsymbol{x} - \boldsymbol{X}(s)\big) + \mu \int_{R}^{\infty} ds \delta^{(3)}\big(\boldsymbol{x} - \boldsymbol{X}(s)\big)$$

$$\int_{-\infty}^{-R} ds \delta^{(3)}\big(\boldsymbol{x} - \boldsymbol{X}(s)\big) = \delta(x) \cdot \big(1 - H(y + R)\big) \cdot \delta(z) \equiv I_1$$

$$\int_{R}^{\infty} ds \delta^{(3)}\big(\boldsymbol{x} - \boldsymbol{X}(s)\big) = \delta(x \cos\theta - y \sin\theta) H(x \sin\theta + y \cos\theta\ - R) \delta(z) \equiv I_2$$

CS with bend

According to the linearized Einstein equation, nonzero components of the energy-momentum tensor give us the nonzero components of the metric perturbation $h_{\mu\nu}$. The geodesics equation for photons:

$$\begin{cases} \dfrac{dv^1}{dx^3} = -\dfrac{1}{2}\dfrac{\partial h_{33}}{\partial x^1} + v^1\dfrac{\partial h_{11}}{\partial x^3} + v^2\dfrac{\partial h_{12}}{\partial x^3} \\ \dfrac{dv^2}{dx^3} = -\dfrac{1}{2}\dfrac{\partial h_{33}}{\partial x^2} + v^1\dfrac{\partial h_{12}}{\partial x^3} + v^2\dfrac{\partial h_{22}}{\partial x^3} \end{cases}$$

$$h_{\mu\nu}(x) = 4G\int d\boldsymbol{x}'\,\frac{S_{\mu\nu}}{|\boldsymbol{x}-\boldsymbol{x}'|},$$

$$S_{\mu\nu} = \begin{pmatrix} 0 & 0 & 0 & 0 \\ 0 & -I_1 - I_2 cos^2\theta & -I_2\sin\theta\cos\theta & 0 \\ 0 & -I_2\sin\theta\cos\theta & -I_2 sin^2\theta & 0 \\ 0 & 0 & 0 & I_1 + I_2 \end{pmatrix}$$

CS with bend

The initial boundary problem for photon trajectory, that should be solved numerically using the shooting method:

$$\begin{cases} \dfrac{d\boldsymbol{v}}{d(z/R_g)} = -\dfrac{1}{2}\nabla_{\boldsymbol{n}}(h_1+h_2) - \left[\dfrac{\partial h_1}{\partial(z/R_g)}\begin{pmatrix} cos^2\theta & \sin\theta\cos\theta \\ \sin\theta\cos\theta & sin^2\theta \end{pmatrix} + \dfrac{\partial h_2}{\partial(z/R_g)}\begin{pmatrix} 1 & 0 \\ 0 & 0 \end{pmatrix}\right]\boldsymbol{v} \\ \dfrac{d\boldsymbol{n}}{\partial(z/R_g)} = \boldsymbol{v} \\ \boldsymbol{n}(z=0) = \boldsymbol{n}_0 \\ \boldsymbol{n}(z=R_g) = \boldsymbol{0} \end{cases}$$

← The relationship between the direction of motion of the photon and the change in its position relative to the visual beam.

$$\boldsymbol{n}\cdot R_g = (x \quad y)$$

$$h_1 \equiv 4G\mu\int d\boldsymbol{x}'\,\frac{\delta(x\cos\theta - y\sin\theta)H(x\sin\theta + y\cos\theta - R)\delta(z)}{|\boldsymbol{x}-\boldsymbol{x}'|}$$

$$h_2 \equiv 4G\mu\int d\boldsymbol{x}'\,\frac{\delta(x)\cdot\big(1-H(y+R)\big)\cdot\delta(z)}{|\boldsymbol{x}-\boldsymbol{x}'|}$$

Bend angle $\theta = 0$

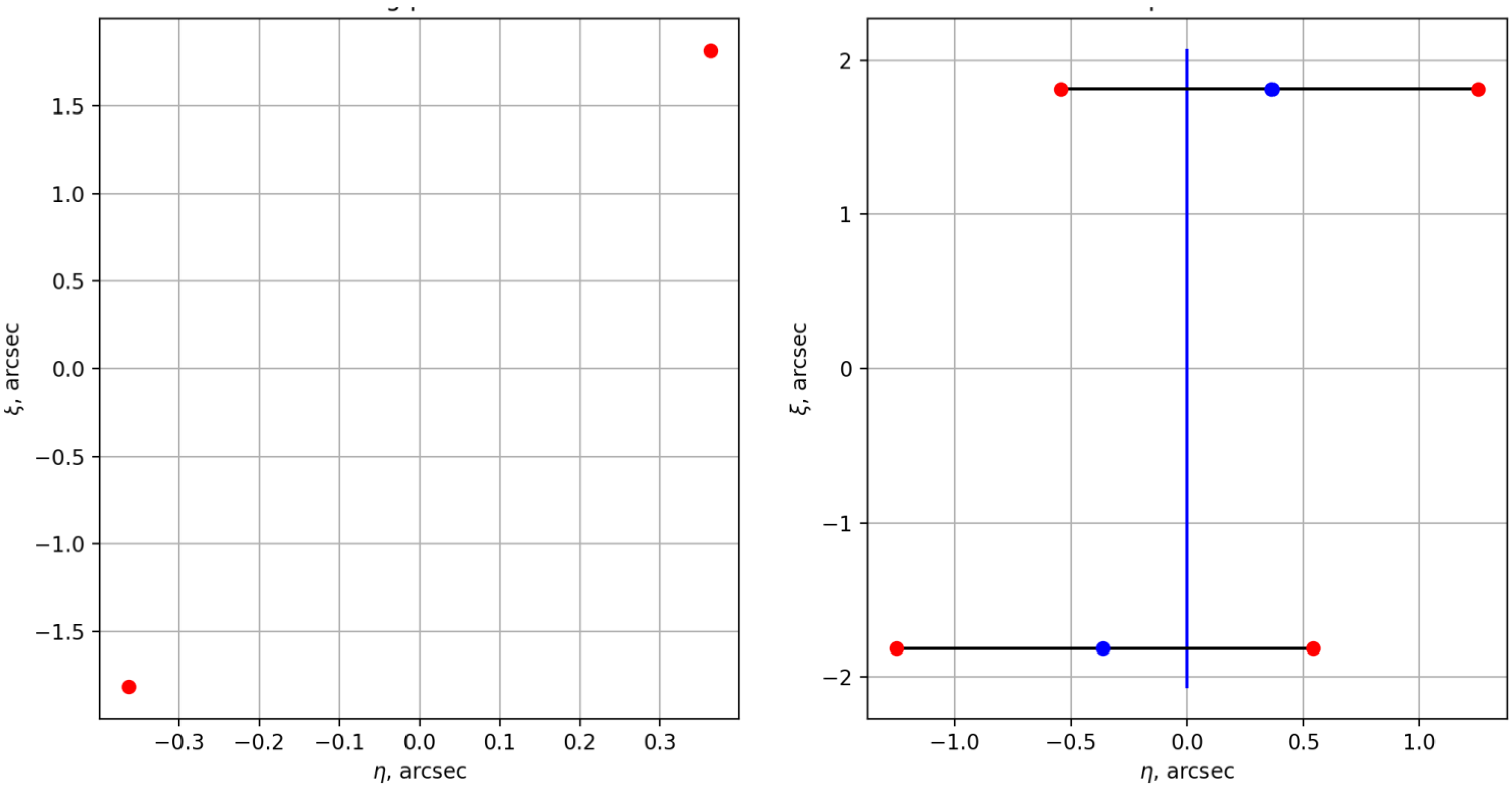

Small bend angle θ

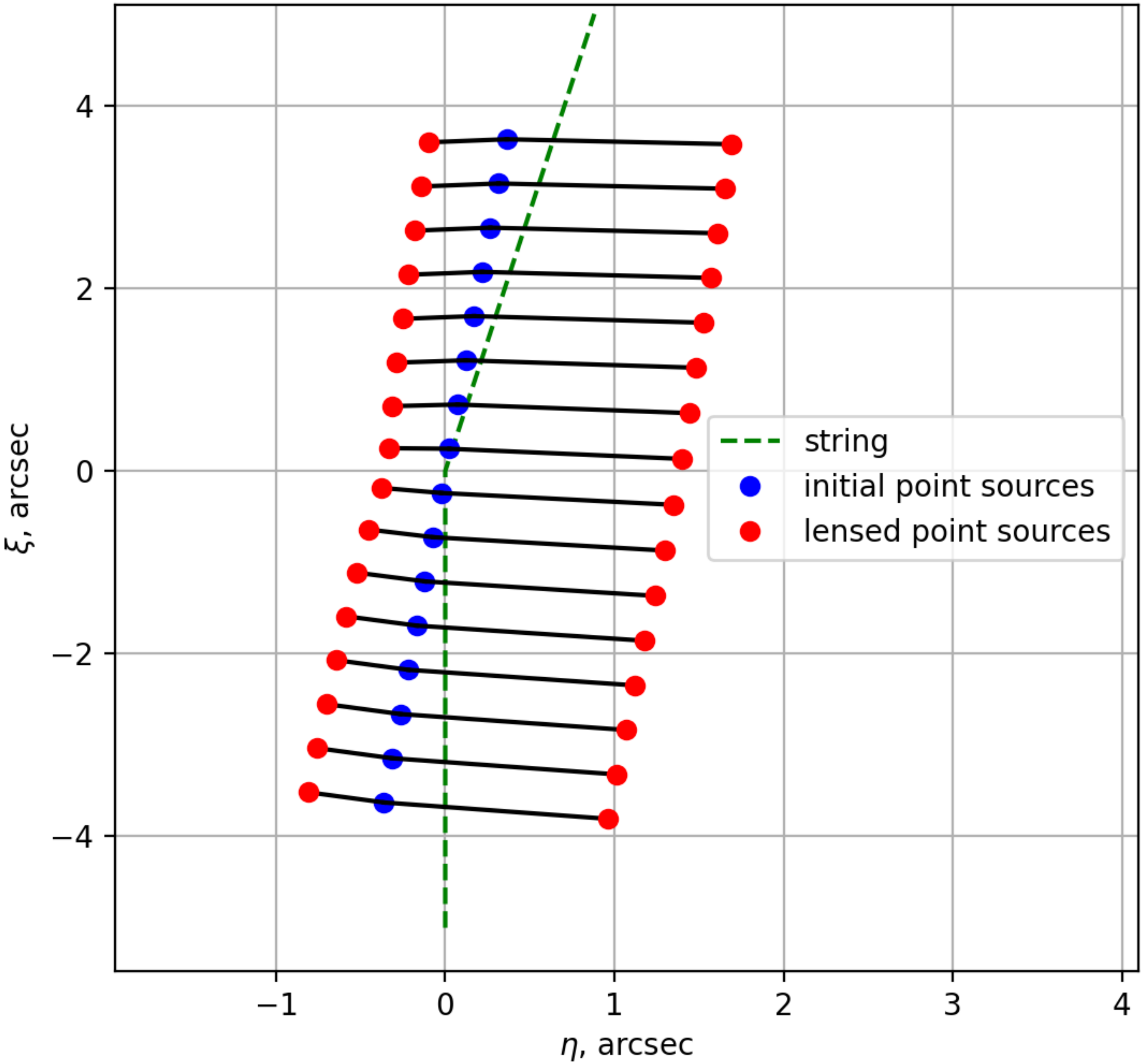

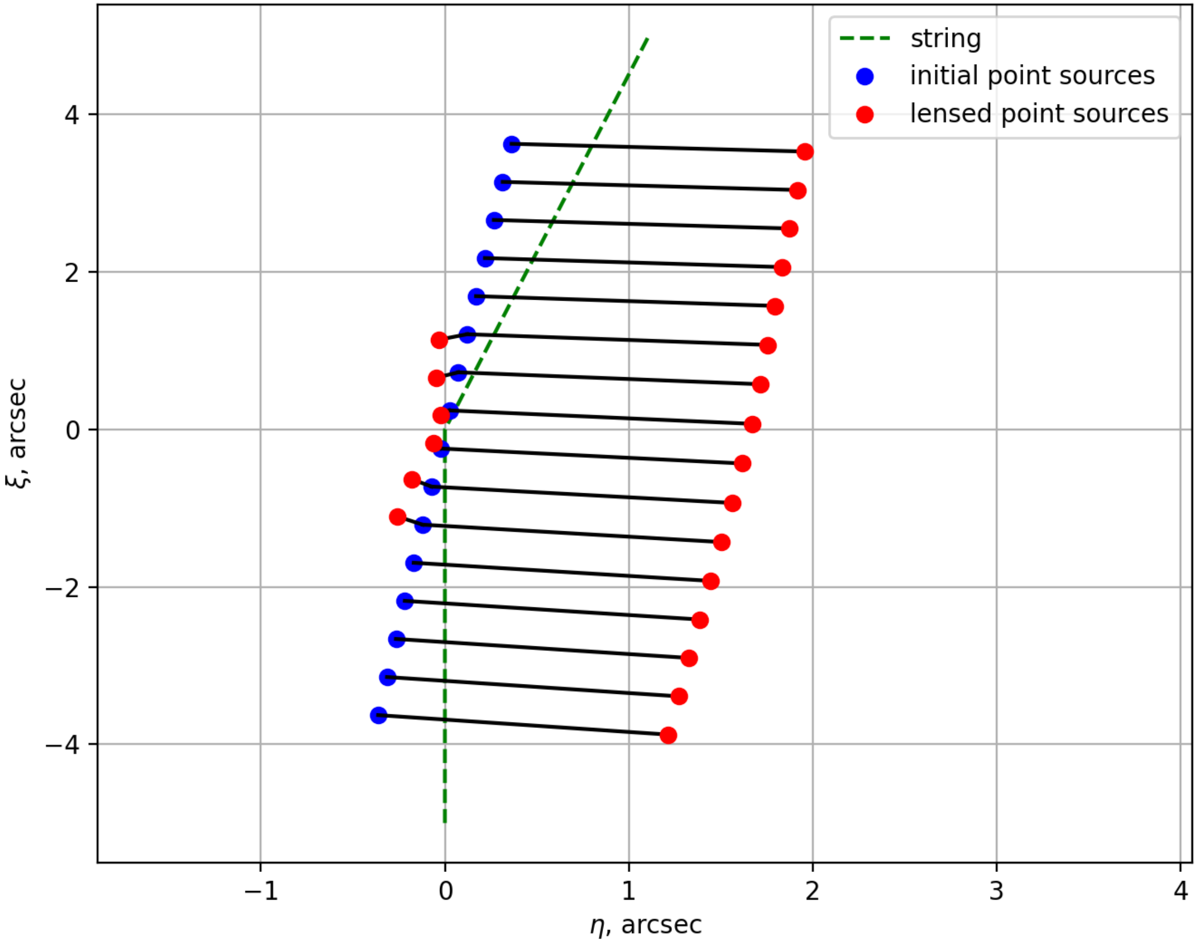

$G\mu = 7{,}0 \cdot 10^{-7}$ and
$Rs/Rg = 0.5$ is $\theta c \approx 13°$.

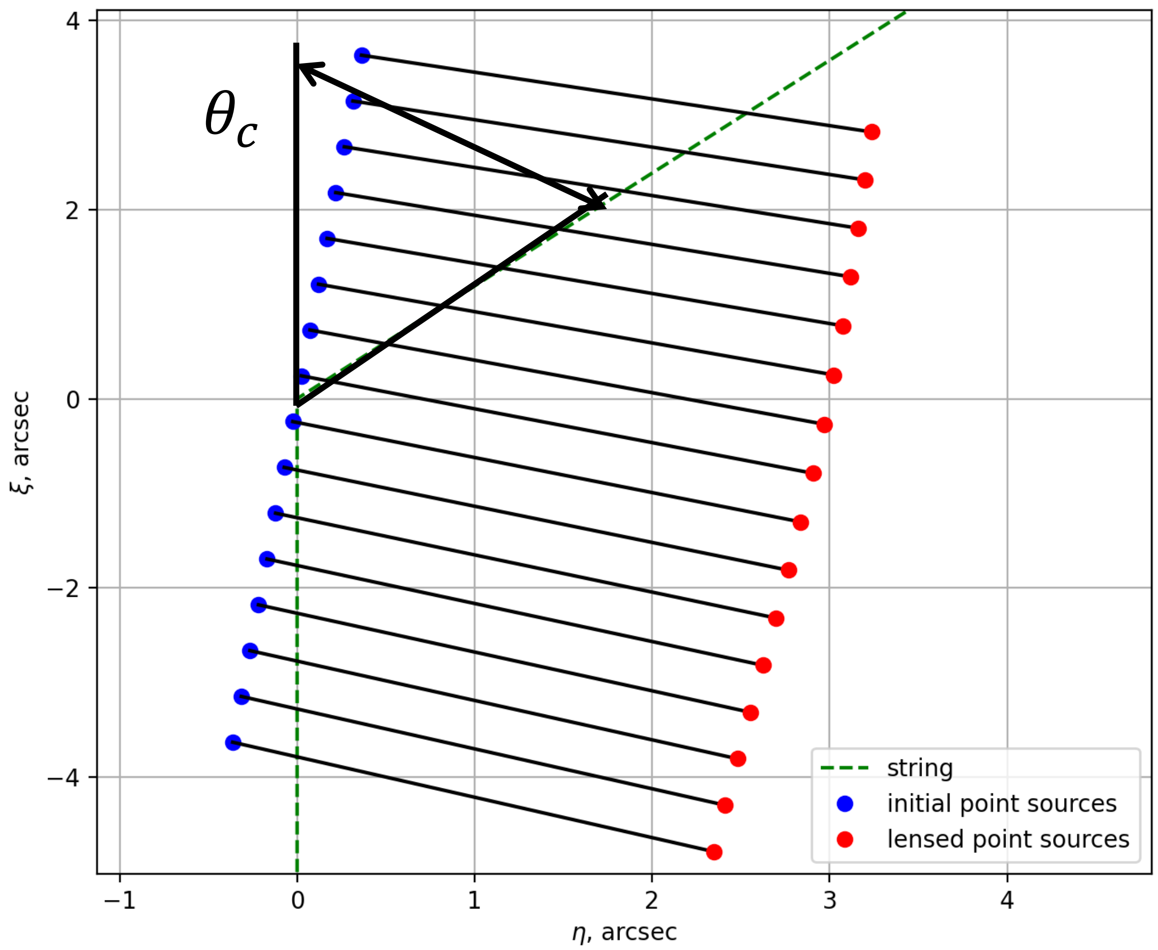

Disappearance of the doubling for $\theta > \theta_c$.
This result can be an argument for the observational lack of double images of galaxies.

The slightest deviation of the CS from the straight line will lead to the loss of a double image.

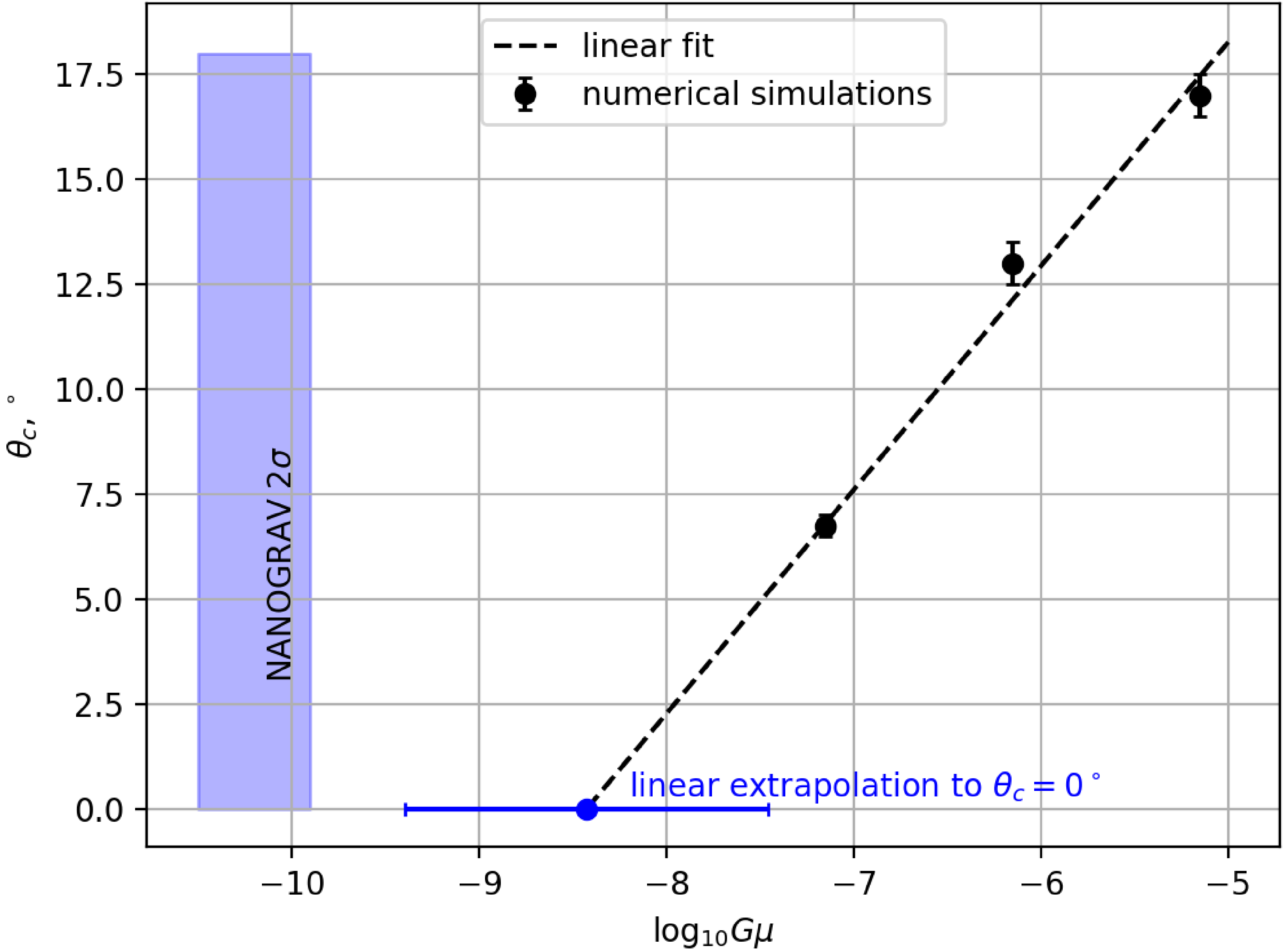

Modern methods of cosmic string detection:

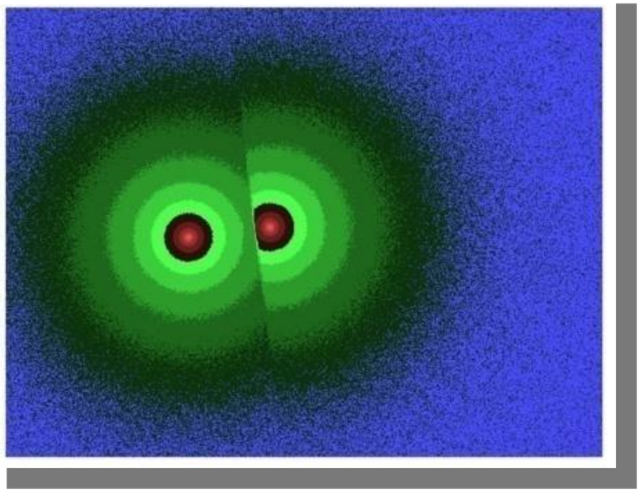

search for special gravitational lensing events (excess in number, isophotes cut etc).

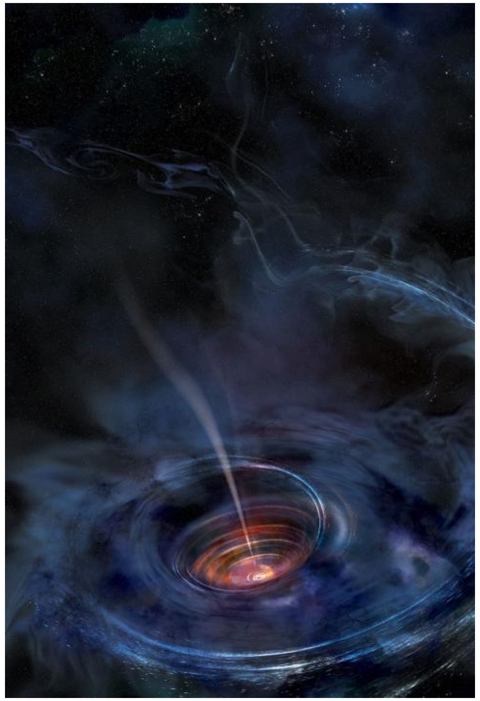

gravitational radiation of CS loops;

the CS-BH, CS-CS interactions;

the decay of heavy particles emitted by a CS;

some model depended exotic methods.

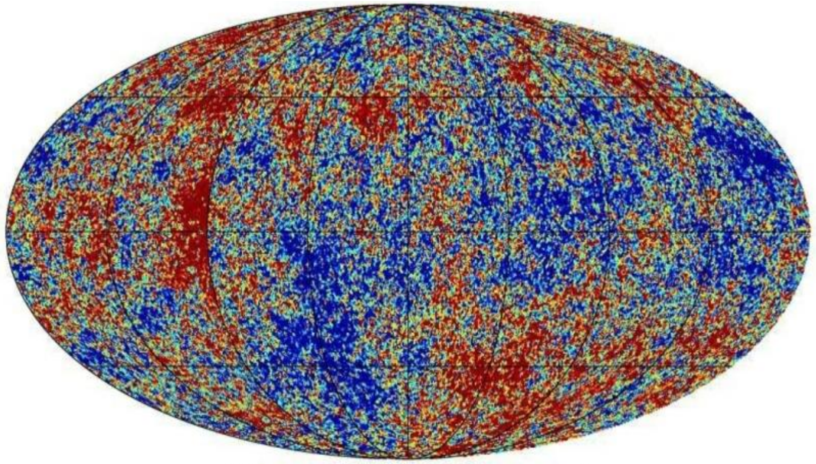

analysis of the anisotropy structure of CMB (WMAP, “Plank” etc).

Kaiser-Stebbins effect of CS in CMB anisotropy

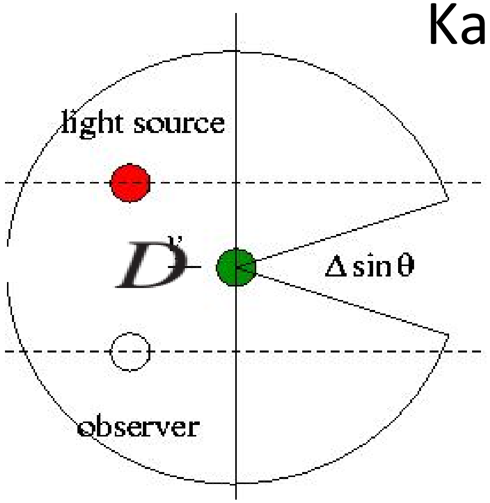

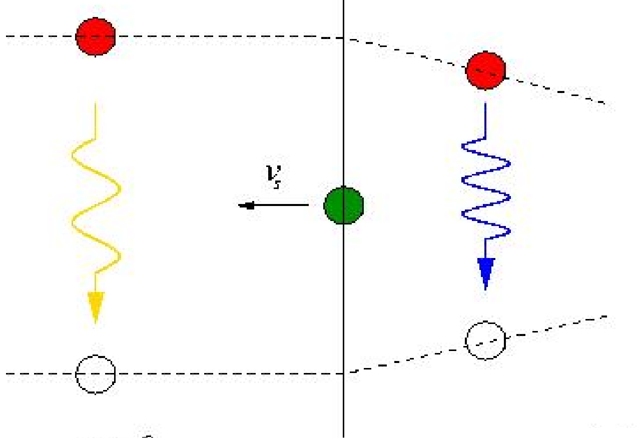

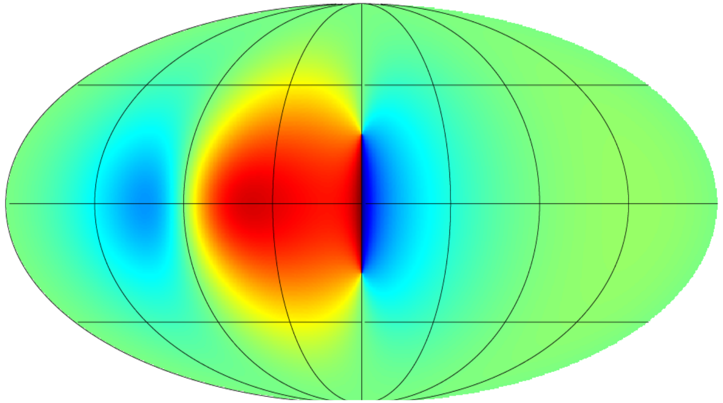

Model of anisotropy induced by single straight CS

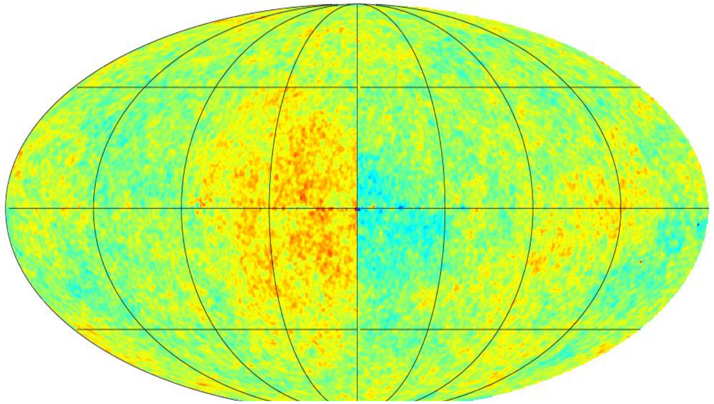

WMAP data + model of anisotropy induced by single straight CS ($\delta T \approx 150\ \mu K$)

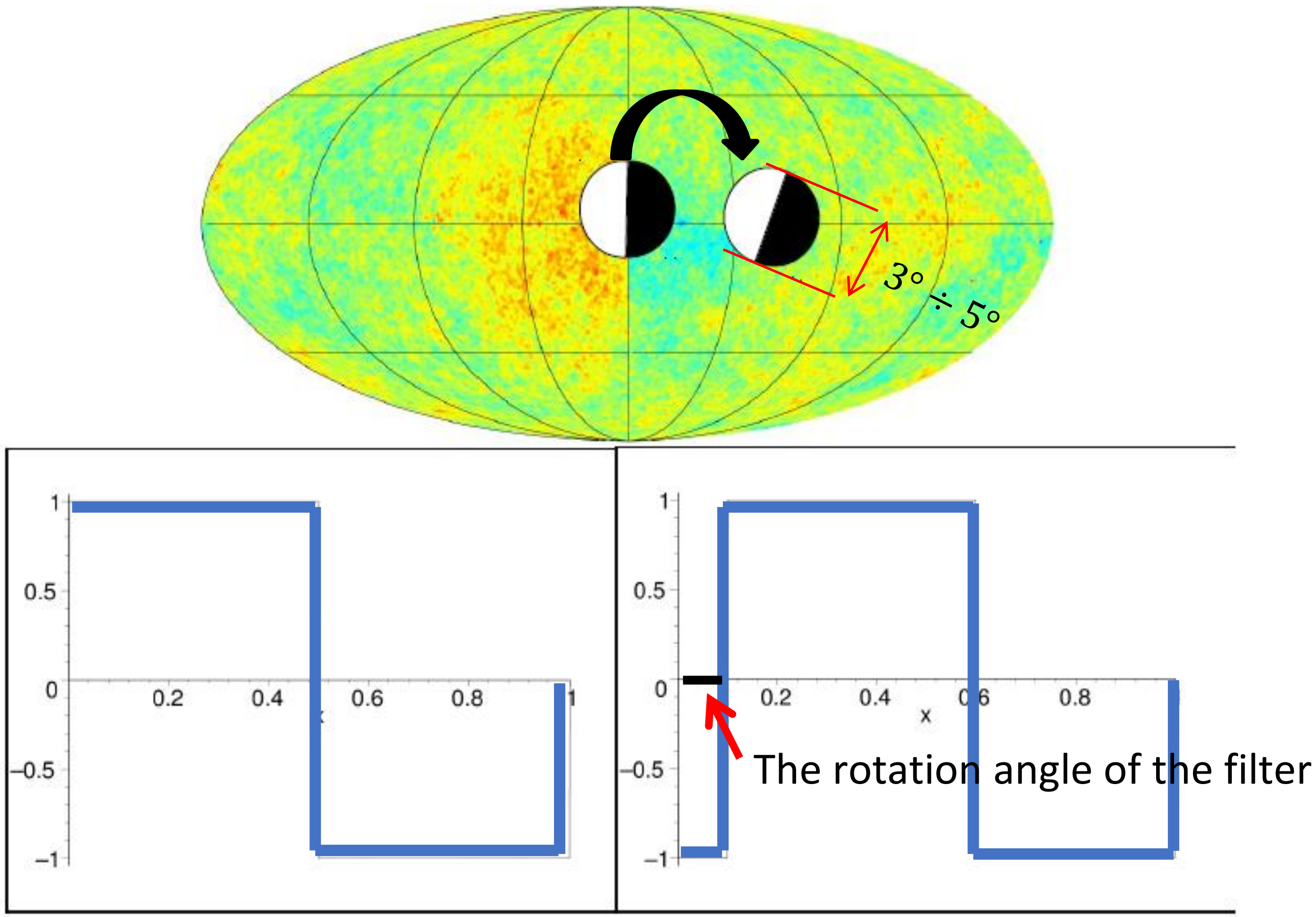

Modified Haar wavelet

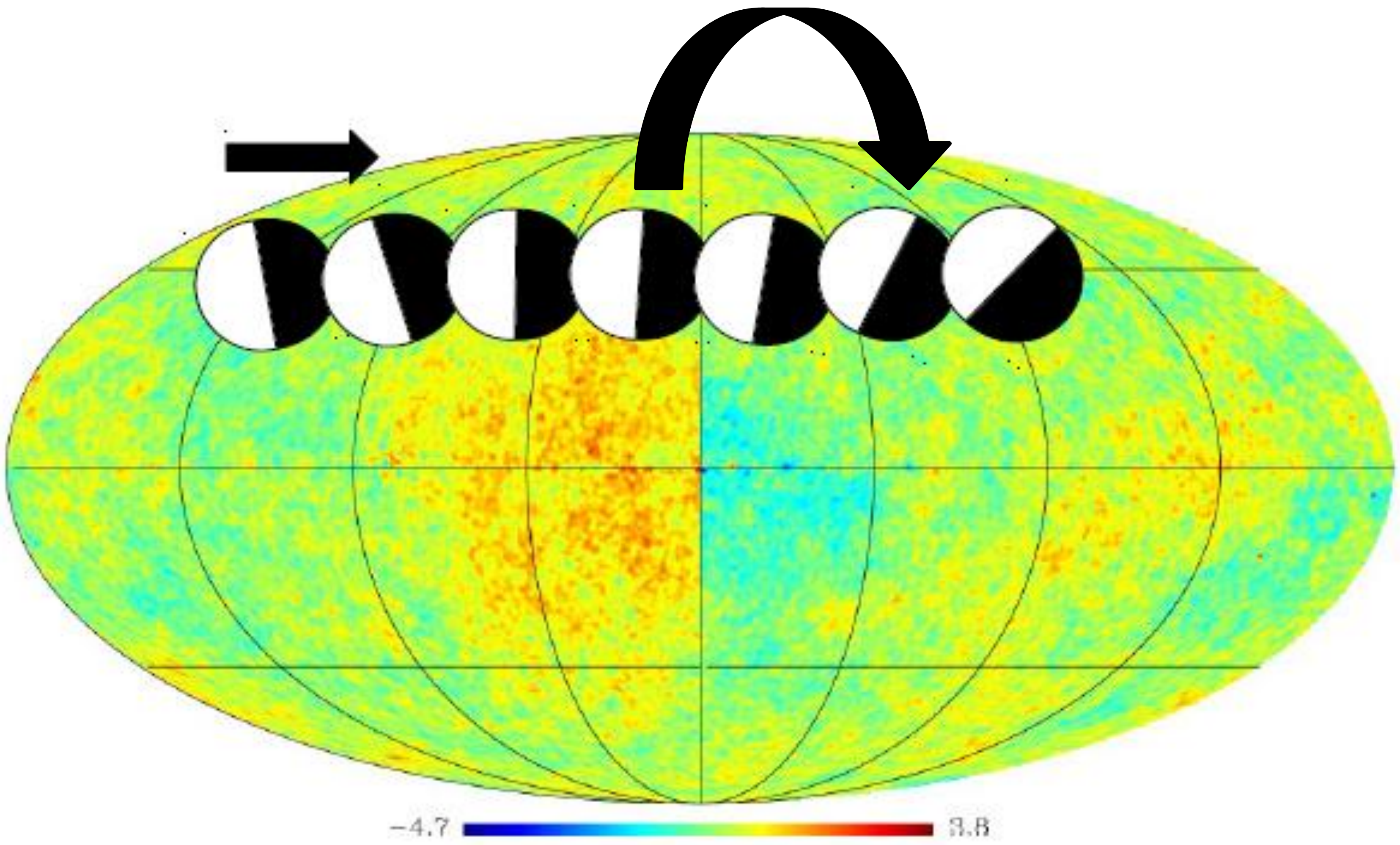

−4.7
3.8

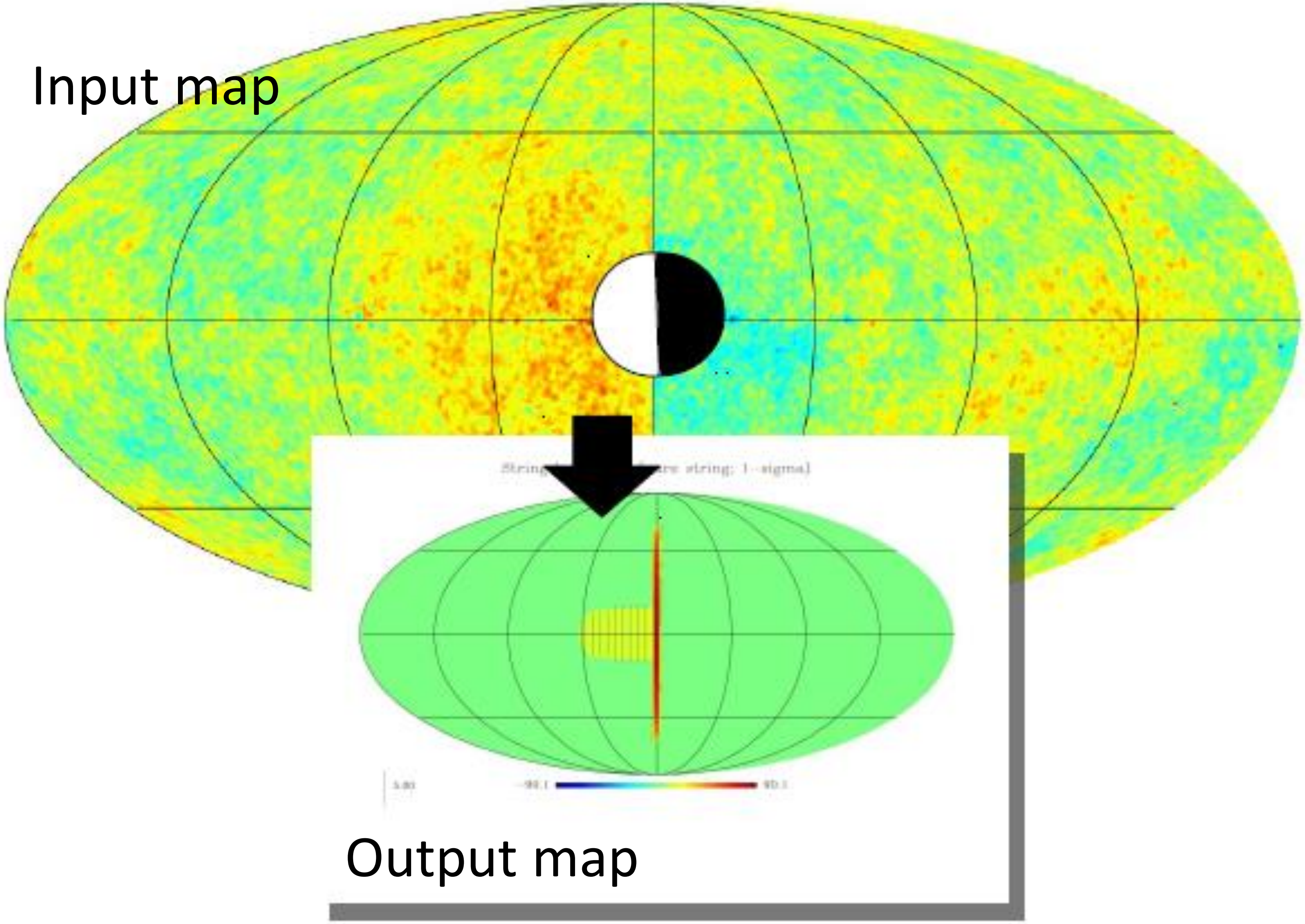
Input map
Output map

The result of processing the CMB data (“Planck”) by the Haar filter

$\delta T \approx 40\ \mu K, \Delta\theta \approx 3''(v = 0{,}9c)$

$\alpha = 11{:}29{:}03, \delta = +15{:}23{:}37;$
$\alpha = 10{:}57{:}47, \delta = +25{:}03{:}51.$

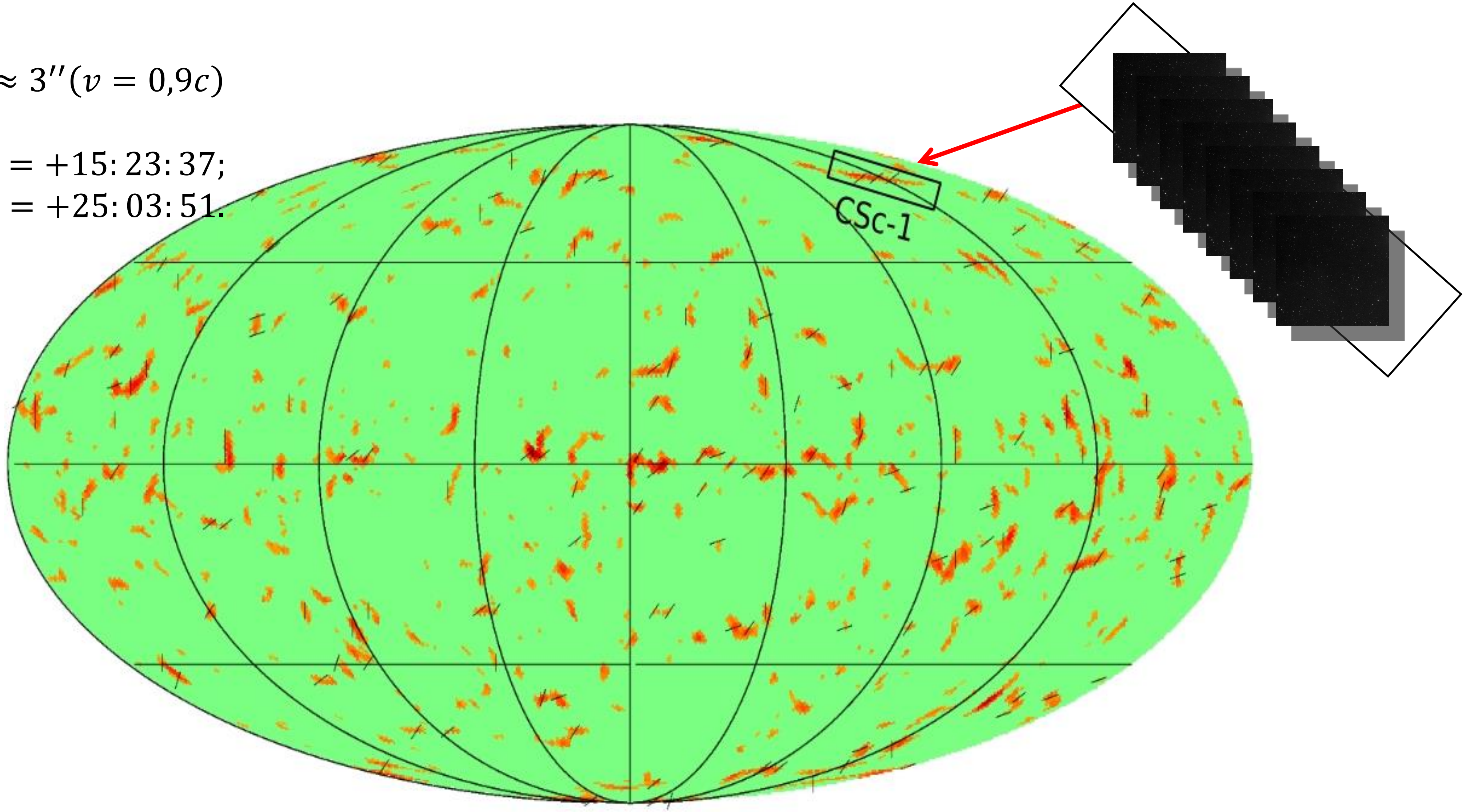

Selection of candidates for GL pairs (automatic, in galaxy catalogs SDSS)

- Angular distance between the components of the pairs [2",9"].
- Identical photometric redshifts.
- The same component intensity ratio in all available frequency bands.

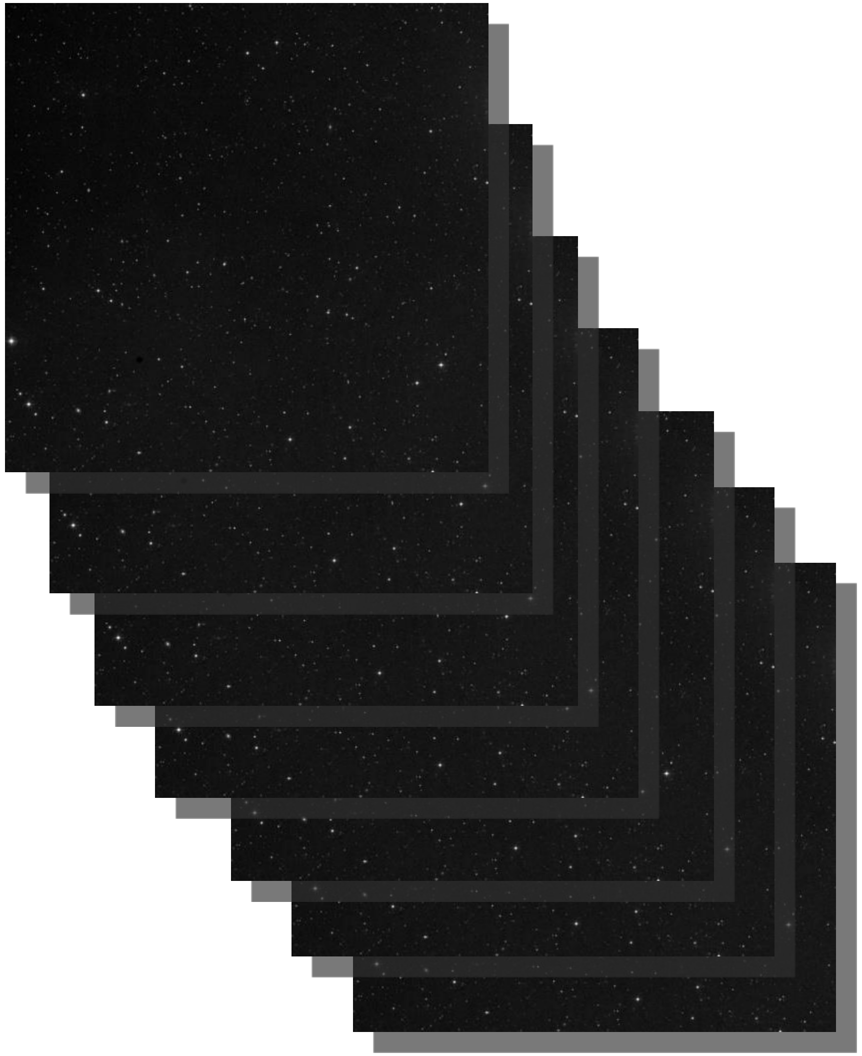

Explore Home
Search
Imaging Summary
FITS
Finding chart
Other Observations
Neighbors
Galaxy Zoo
PhotoTag
Field
Frame
PhotoObj
PhotoZ
Cross-ID
Spec Summary
All Spectra
NED search
SIMBAD search
ADS search
Notes
Save in Notes
Show Notes
Print

Not logged in | Help | Login

Type	run	rerun	camcol	field	obj	SDSS Object ID
GALAXY	5183	301	6	240	177	1237667736649203889

RA, Dec		Galactic Coordinates (*l*, *b*)	
Decimal	Sexagesimal	*l*	*b*
167.362011215, 22.659893665	11:09:26.88, +22:39:35.61	218.242868481	66.487111818

Imaging

Flags	DEBLENDED_AT_EDGE STATIONARY BINNED1 INTERP COSMIC_RAY MANYPETRO CHILD

6 filters

Magnitudes				
u	g	r	i	z
22.19	20.75	19.10	18.55	18.26

Magnitude uncertainties				
err_u	err_g	err_r	err_i	err_z
0.35	0.04	0.02	0.02	0.04

1σ-error

Image MJD	mode	Other observations	parentID	nChild	extinction_r	PetroRad_r (arcsec)
53439	PRIMARY	0	1237667736649203888	0	0.04	3.85 ± 0.571

Mjd-Date	photoZ (KD-tree method)	Galaxy Zoo 1 morphology
03/10/2005	0.330 ± 0.0256	-

photometric redshift

Comparison of the distribution of gravitational lensing pairs in areas where there are no CS candidates (“control fields”) with a field where there is a CS candidate (“string field”).

We found a statistically significant excess of **22%** (per 1 sq. deg.) of the number of candidate pairs for gravitational-lens events in CS field compared with control fields (3σ, 1300 pairs).

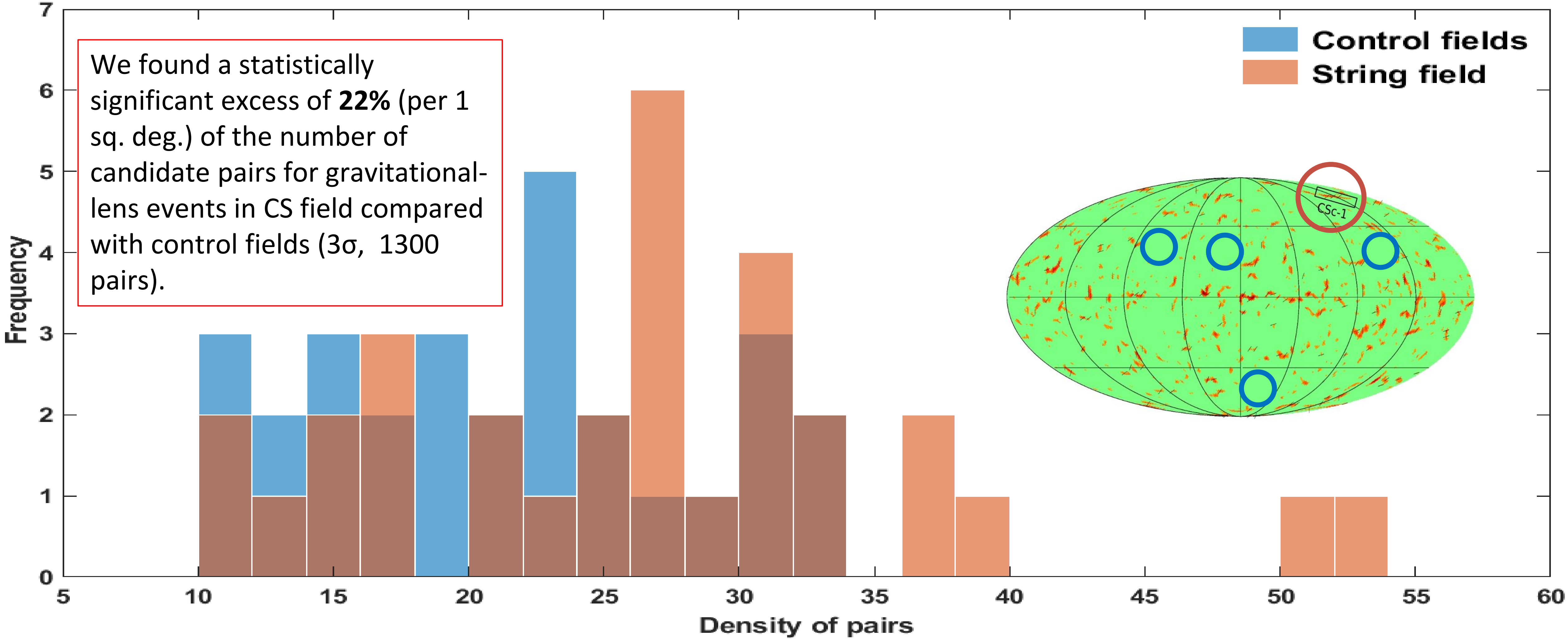

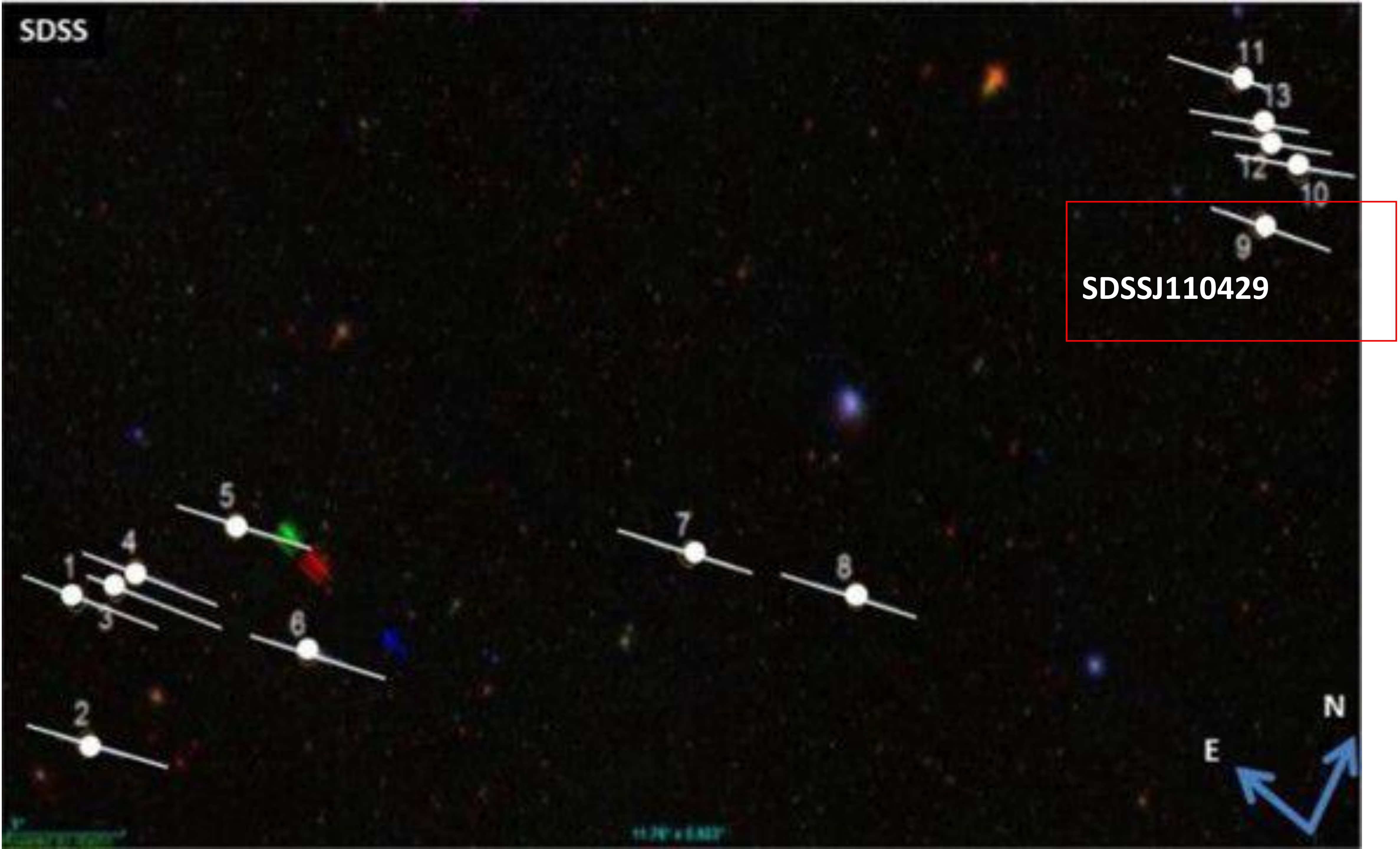

SDSS
11
13
12
10
9
SDSSJ110429
5
4
1
3
6
7
8
2
N
E

Object SDSS J110429 (7.03.2022 observations)

Himalayan Chandra Telescope of the Indian Astronomical Observatory (IAO), located at 4500 m above sea level; D = 2,0 m

0.296′′/pix

MAST Pan-STARRS 1
0.25′′/pix

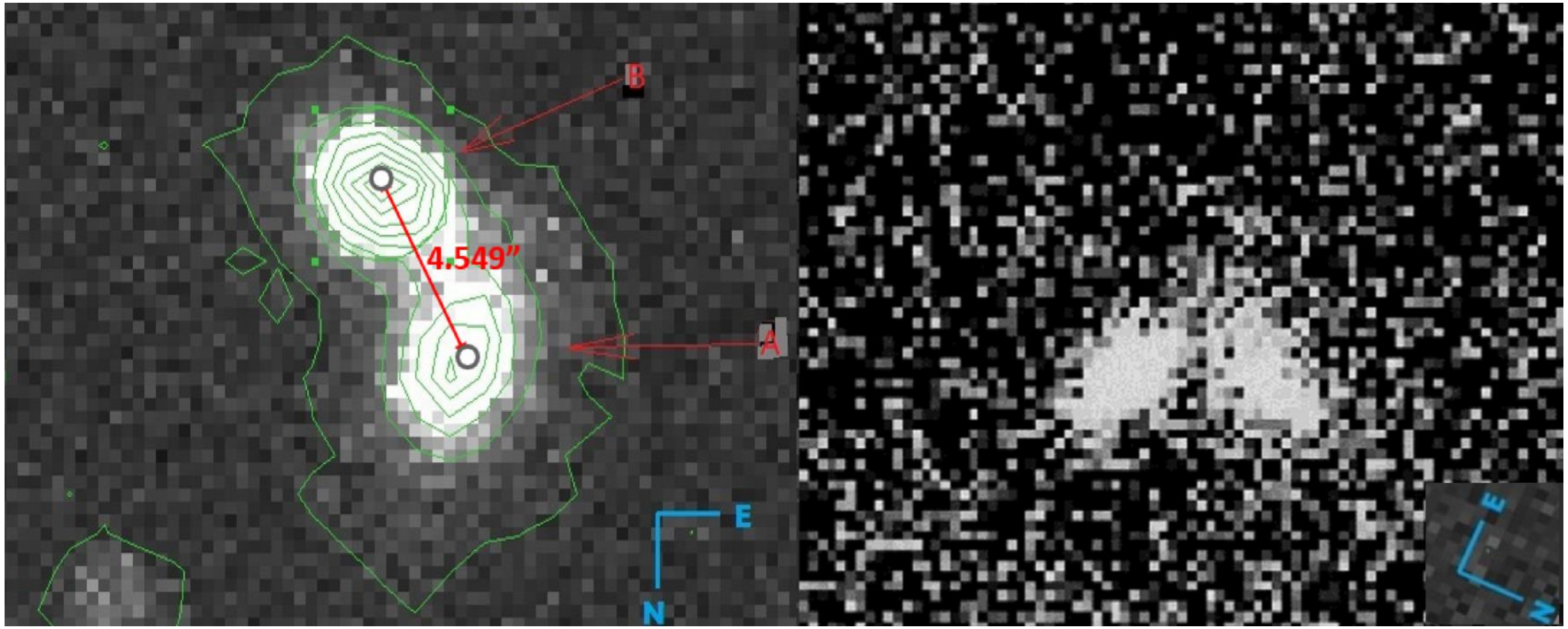

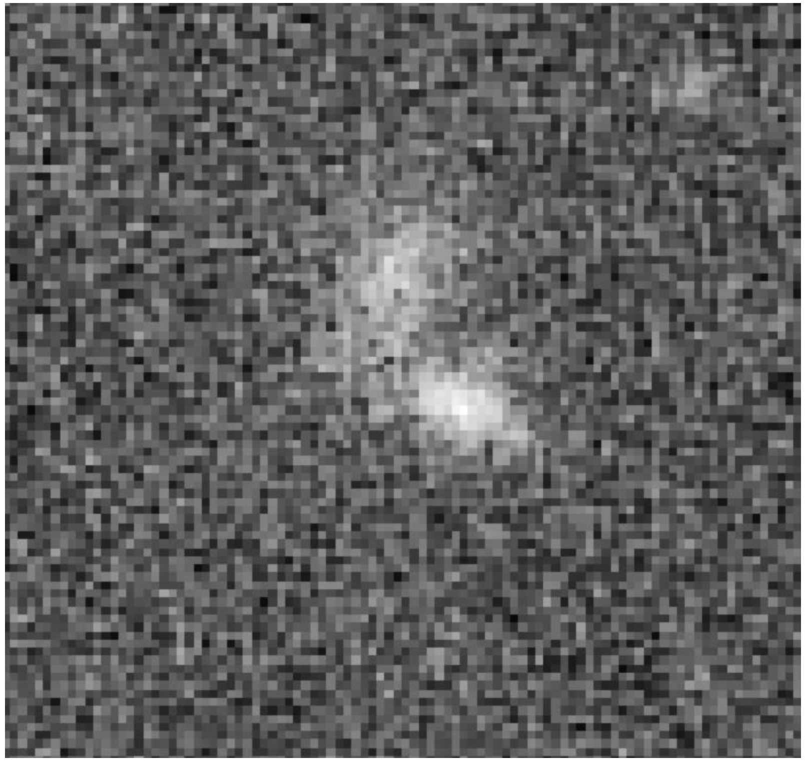

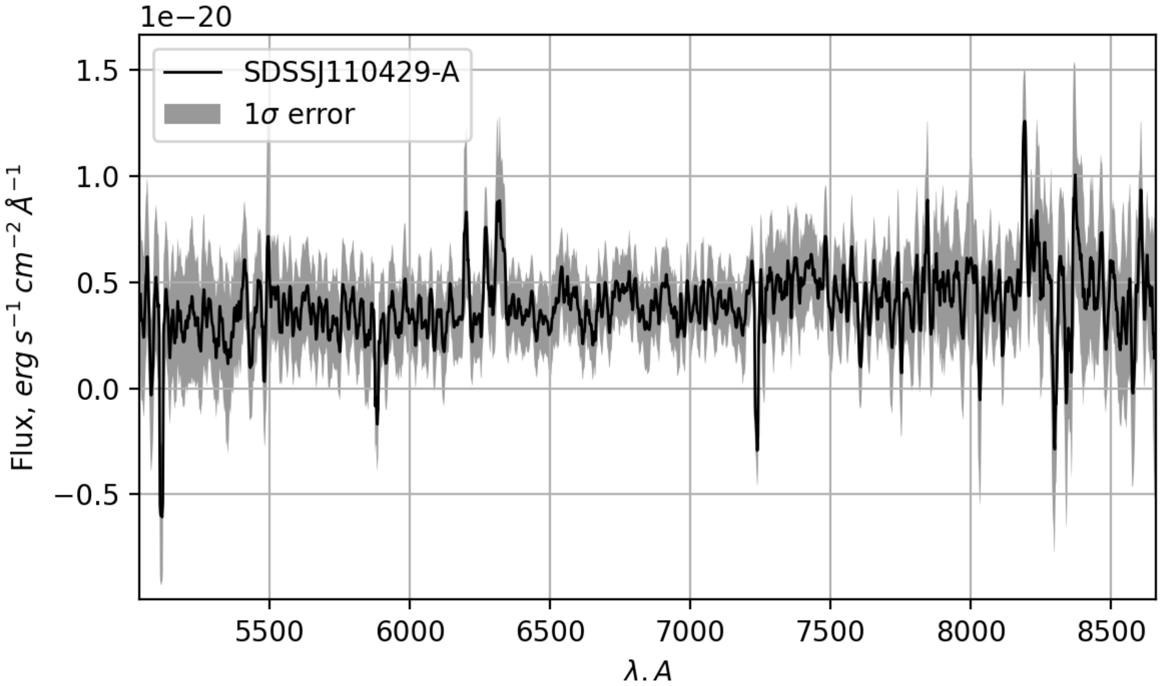

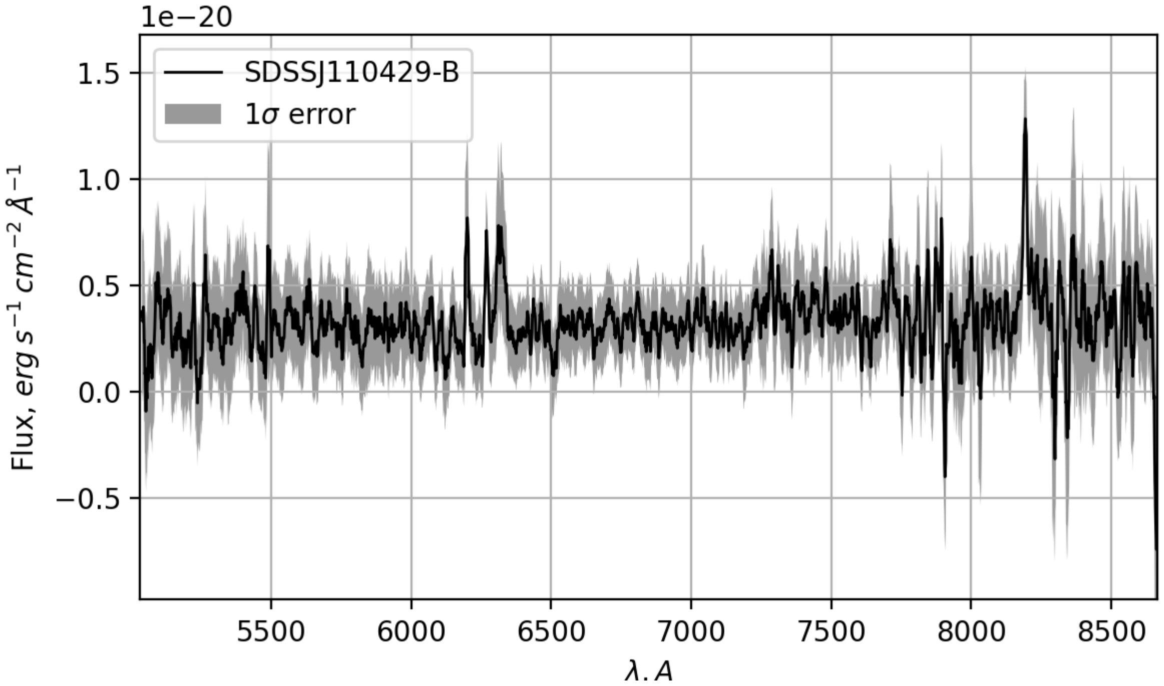

Smoothing on the scale $\delta\lambda = 3.6$ Å

$z = 0{,}236$

$p = 90\%$

$(\mathrm{N} = 1000; \mathrm{Pearson}\backslash\mathrm{Spearman}\backslash\mathrm{Kendall}\ r: 0{,}571\backslash 0{,}613\backslash 0{,}447)$

Strong indication on gravitational nature of two components.

Several lines (Hα , Hβ , [OIII]λ 5007, [NII]λ 6583, [SII]λ 6718, [SII]λ 6733 and [OI]λ 6300) were identified and fitted by a Gaussian profile. In order to analyze the properties of spectra without the noisy continuum, $\chi 2$ criteria was calculated for profiles of strongest lines Hα , Hβ and [OIII]λ 5007, and for the widths of all lines. Identity with p-value **90%**.

$$\frac{G\mu}{c^2} = 0.05$$

$$i = 89.9995°$$

$$R_s \backslash R_g = 0{,}31$$

GUT ($> 10^{16} GeV$) cosmic string? non topological cosmic string?

$v \ll c$; rejection of the concept of relativistic cosmic strings?

$$\frac{\delta T}{T} \approx G\mu\gamma \cdot \frac{v}{c}$$

$$\delta T \approx 38\ \mu K$$

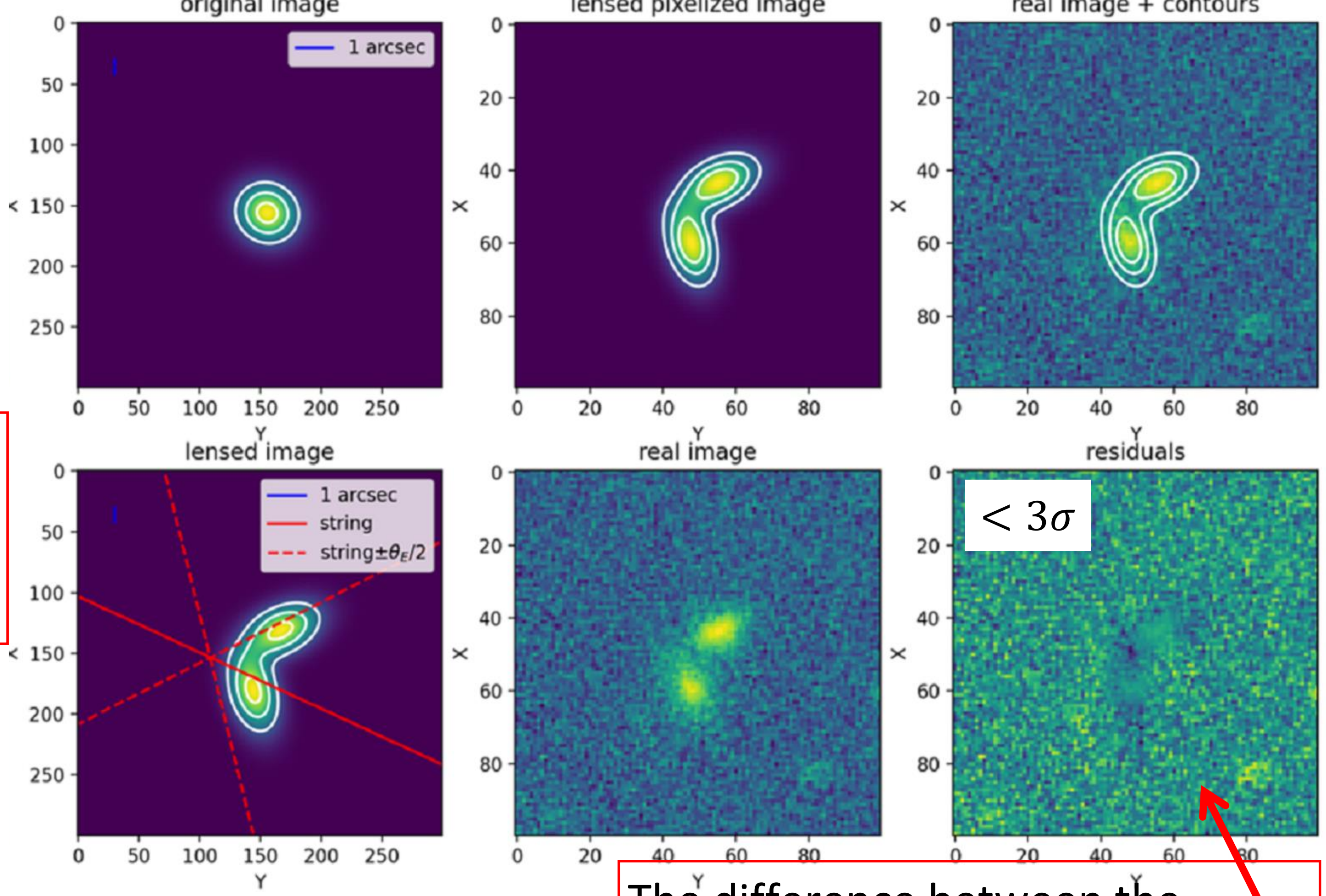

The difference between the gravitational lensing model of a galaxy on an inclined cosmic string and the observational data of the object SDSS J110429

$$\chi^2 = \sum_{i,j} \frac{\left(\left(I^{(model)} * PSF\right)_{ij} - I_{ij}{}^{(observation)}\right)^2}{\sigma_{ij}{}^2}$$

Cosmic string in inflation epoch

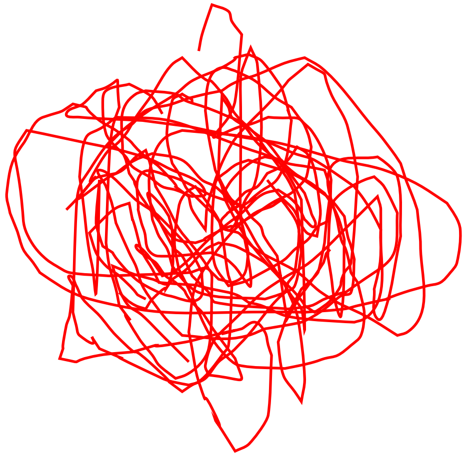

Cosmic string born in inflation epoch, in modern Universe

$i \approx 90°$

$G\mu/c^2 \gg 10^{-7}$

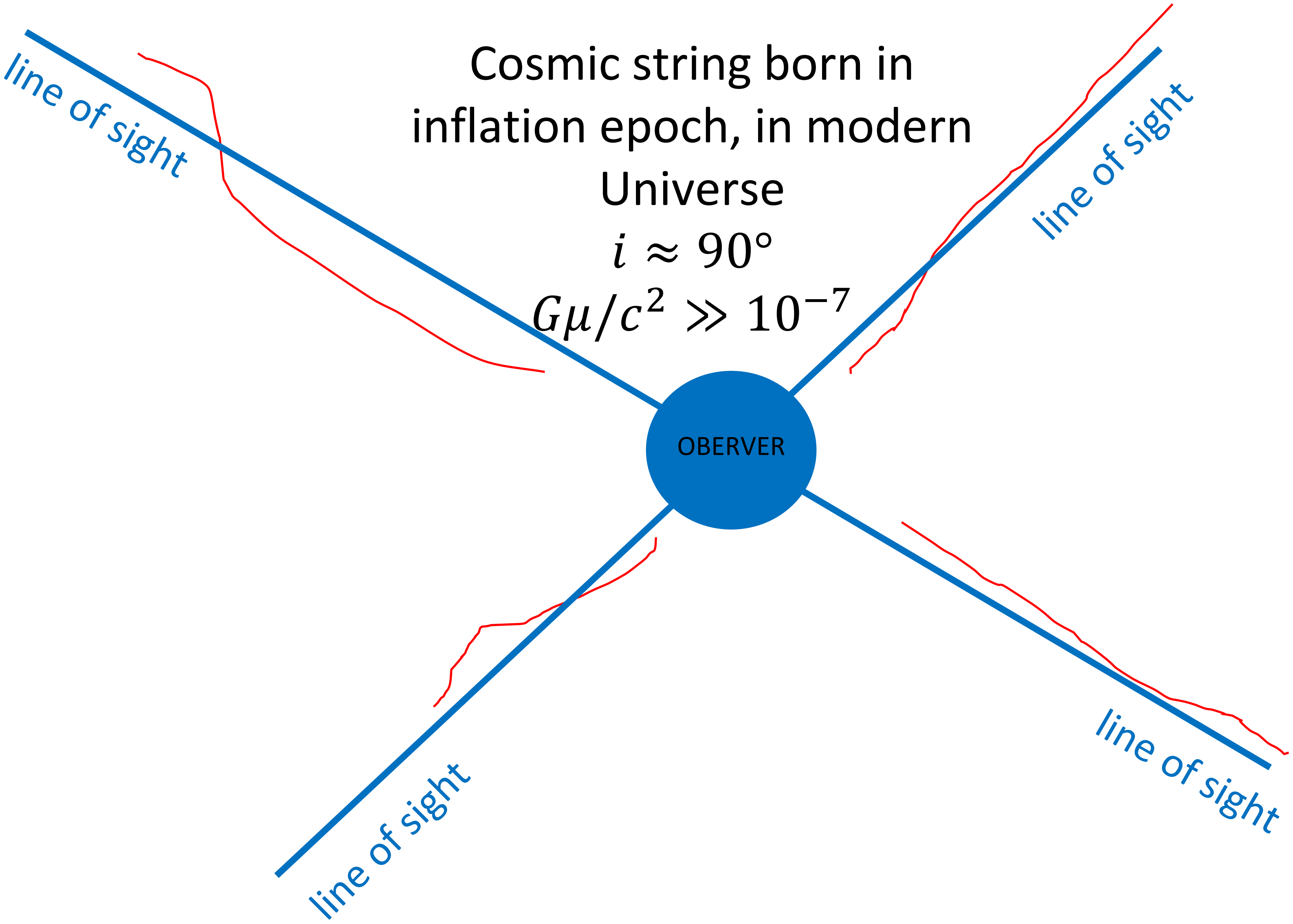

inflationary and heavy cosmic string?

$$\frac{G\mu}{c^2} = 0.01$$
$$i = 89.990°$$

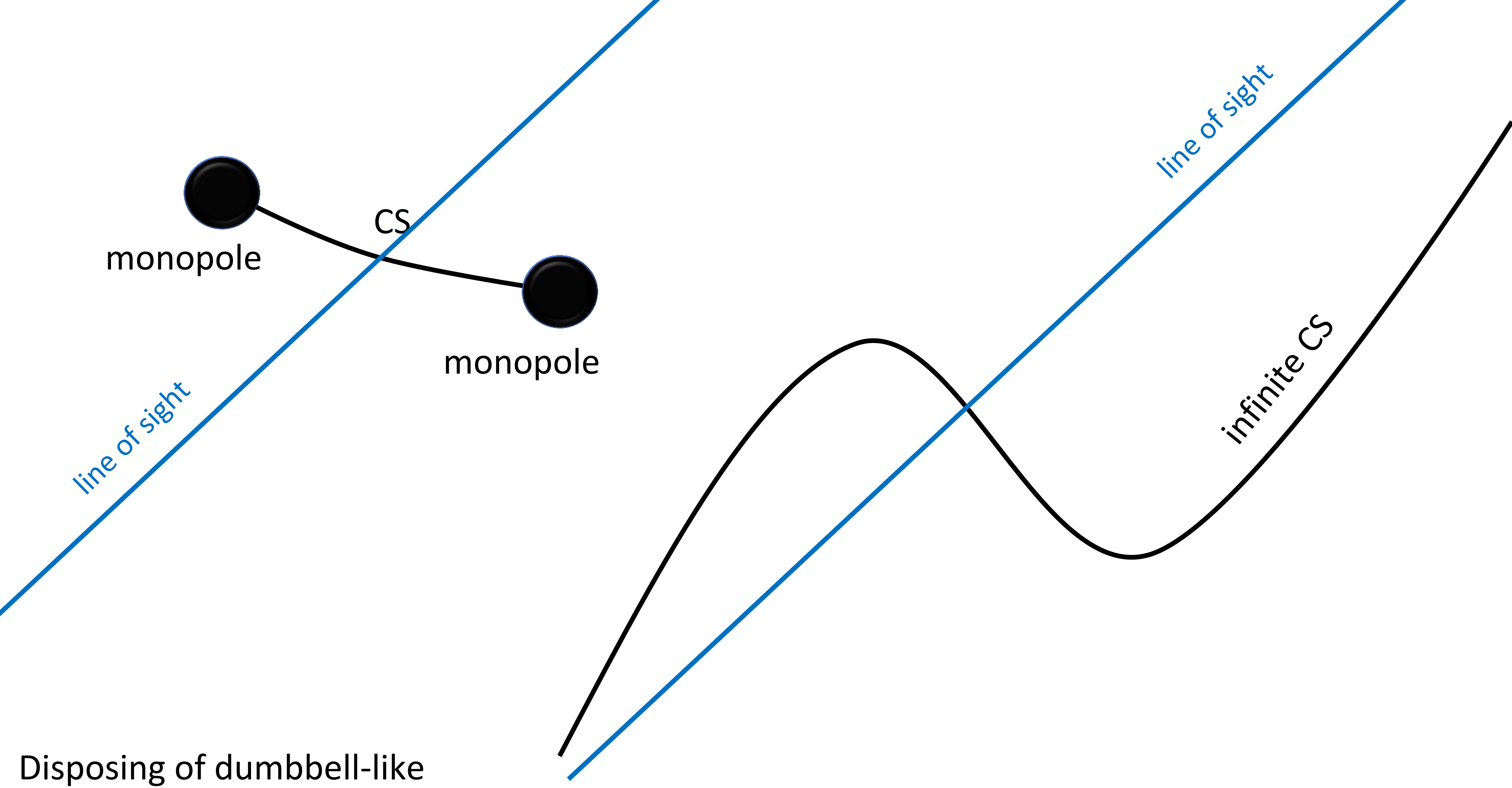

Disposing of dumbbell-like cosmic strings

Preliminary results

1. **THEORY.** It was constracted the gravitation lensing model for *infinite straight* and *thin* CS, **inclined** (analitically) and **with bending** (numerically).

2. The concept of the **critical angle** was introduced: it is found that at large bending angles, the double image disappears, which can serve as an argument for the fact that so few doubled images have been found using CS network paradigm.

3. **OBSERVATIONS.** Photometric and spectroscopic data have been obtained for the gravitational lensing double candidate (SDSS J110429). A quantitative assessment of the probability of the hypothesis that SDSS J110429 is the result of gravitational lensing on inclined cosmic string has been carried out. The difference between the observations and the model is less than 3σ. The spectra and single lines match with accuracy 90%. **SDSS J110429 double object is confirmed as a CS consequence by two independend methods (CMB, gravitational lensing).**

ALL TOGETHER: CS network models are not able to identify gravitational lensing pairs because of the critical angle. Gravitational-wave background observations cannot “see” CS without oscillating loops. There are no theoretical limits on CS velocities. The limitation on the total mass of CS in the Universe (WMAP, “Planck”) does not give estimates of their number. Disposing of dumbbell-like CS. Thus, **promising models are single strings, specially single heavy strings, which could be formed in the inflation epoch or could be non-topological.**